Supporting Information

Template-assisted design of monomeric polyQ models to unravel the unique role of glutamine side chains in disease-related aggregation

Ho-Wah Siu, Benjamin Heck, Michael Kovermann*, Karin Hauser*

Department of Chemistry, University of Konstanz, 78457 Konstanz, Germany

* Correspondence:

michael.kovermann@uni-konstanz.de; karin.hauser@uni-konstanz.de

High-resolution NMR data

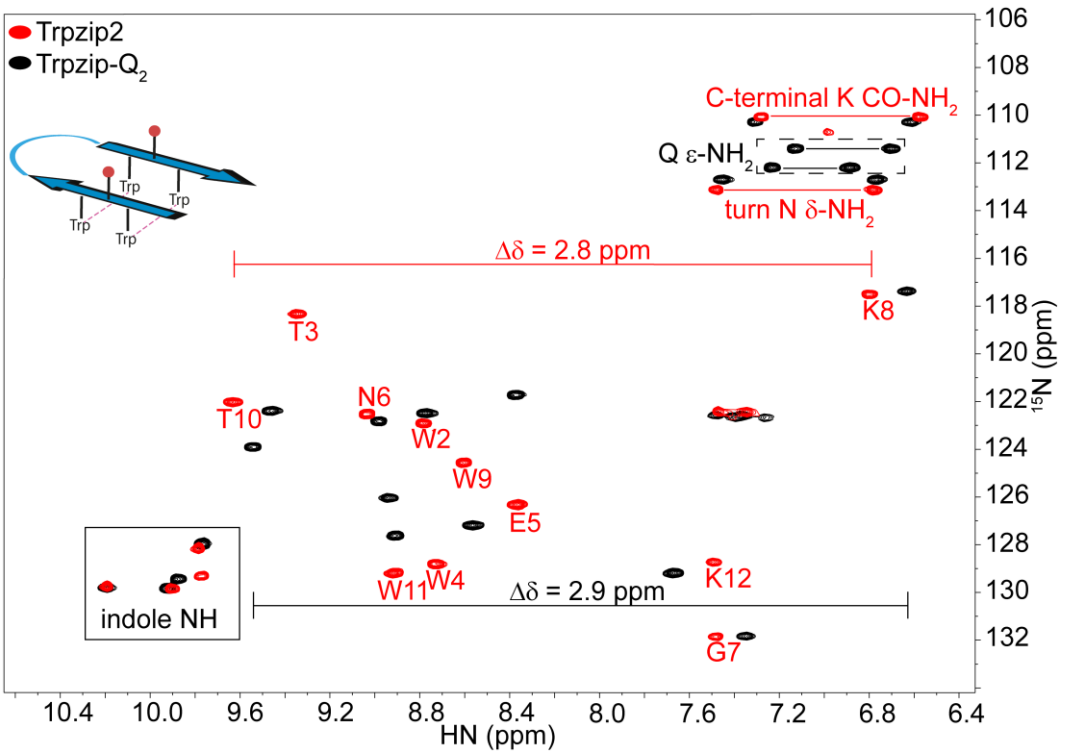

Figure S1a: Two-dimensional ^{1}H-^{15}N HSQC spectra of Trpzip-Q_2 (black) measured at c = 2.2 mM (c = 3.7 mg mL^{-1}) and the template Trpzip2 (red) measured at c = 1.4 mM (c = 2.2 mg mL^{-1}). The dispersion of chemical shifts, $\Delta\delta$, observed for backbone amide protons comprising Trpzip2 ($\Delta\delta$ = 2.8 ppm) and Trpzip-Q_2 ($\Delta\delta$ = 2.9 ppm) is similar indicating a similar peptide fold. The resonance signals of indole NHs comprising tryptophan residues (black frame) remain well dispersed, supporting that the Trp-Trp cross-strand interactions of the two Trp pairs are similar to the template. Both peptides show two pairs of well dispersed cross signals of the C-terminal lysine CO-NH_2 and the side chain amide of asparagine δ-NH_2 (turn). Additionally, Trpzip-Q_2 reveals two pairs of well dispersed signals caused by amide protons of glutamine side chains Q ε-NH_2 (highlighted using a black frame, dashed mode).

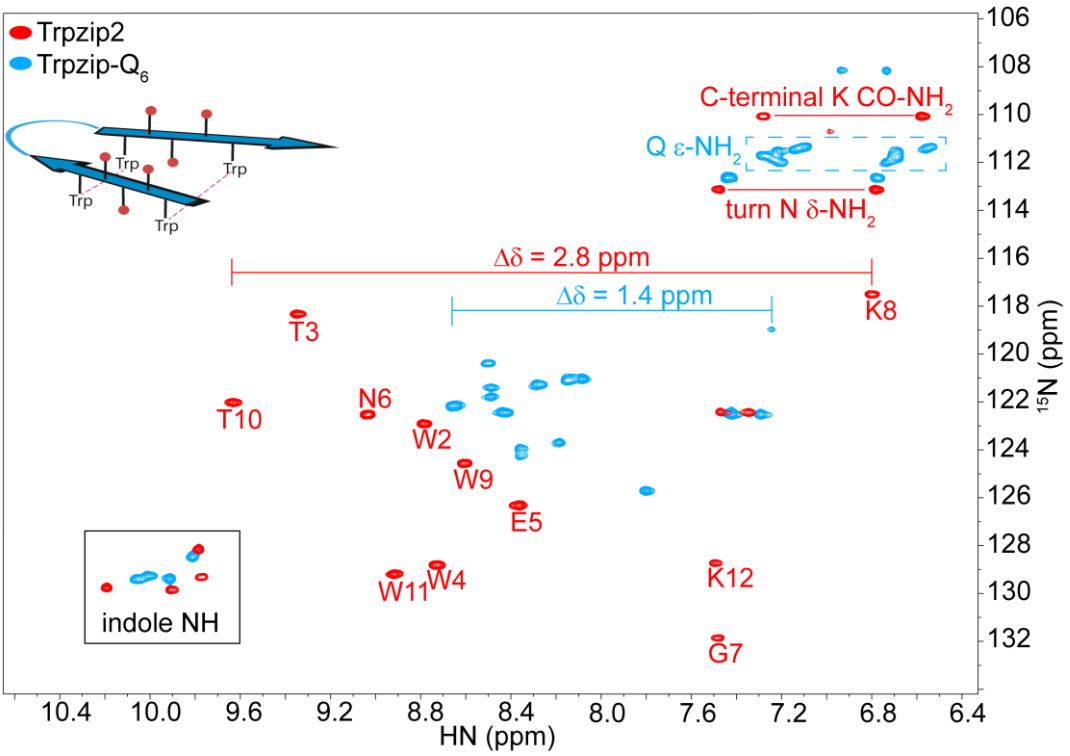

Figure S1b: Two-dimensional ^{1}H-^{15}N-HSQC spectra of Trpzip-Q_6 (blue) measured at c = 0.9 mM (c = 1.9 mg mL^{-1}) and the template Trpzip2 (red) measured at c = 1.4 mM (c = 2.2 mg mL^{-1}). The dispersion of chemical shifts, $\Delta\delta$, observed for backbone amide protons of Trpzip-Q_6 ($\Delta\delta$ = 1.4 ppm) is half compared to Trpzip2 ($\Delta\delta$ = 2.8 ppm) indicating significant conformational changes caused by the insertion of glutamines. The 4 resonance signals of indole NHs comprising tryptophan residues (black frame) are less dispersed with 2 signals overlapping. We assume that the Trp-Trp cross-strand interactions are weaker, but still sufficient to maintain the hairpin structure. There are two pairs of well dispersed cross signals of the C-terminal lysine CO-NH_2 and the turn asparagine δ-NH_2, but with remarkable less dispersed C-terminal lysine signals compared to the template Trpzip2 indicating a more disordered, frayed C-terminus. Additionally, Trpzip-Q_6 reveals signals caused by amide protons of glutamine side chains Q ε-NH_2 which are significantly overlapping (highlighted using a blue frame, dashed mode). The overlap hints similar chemical environments for some of the side chains within the glutamine sequences. We interpret the glutamine-induced conformational change of the backbone, the more disordered C-terminus and the loss of cross-strand tryptophan interactions in such a way that Trpzip-Q_6 adopts a less ordered structure than the template Trpzip2, but with tryptophan interactions effective enough to keep the peptide sequence in a (distorted) hairpin structure.

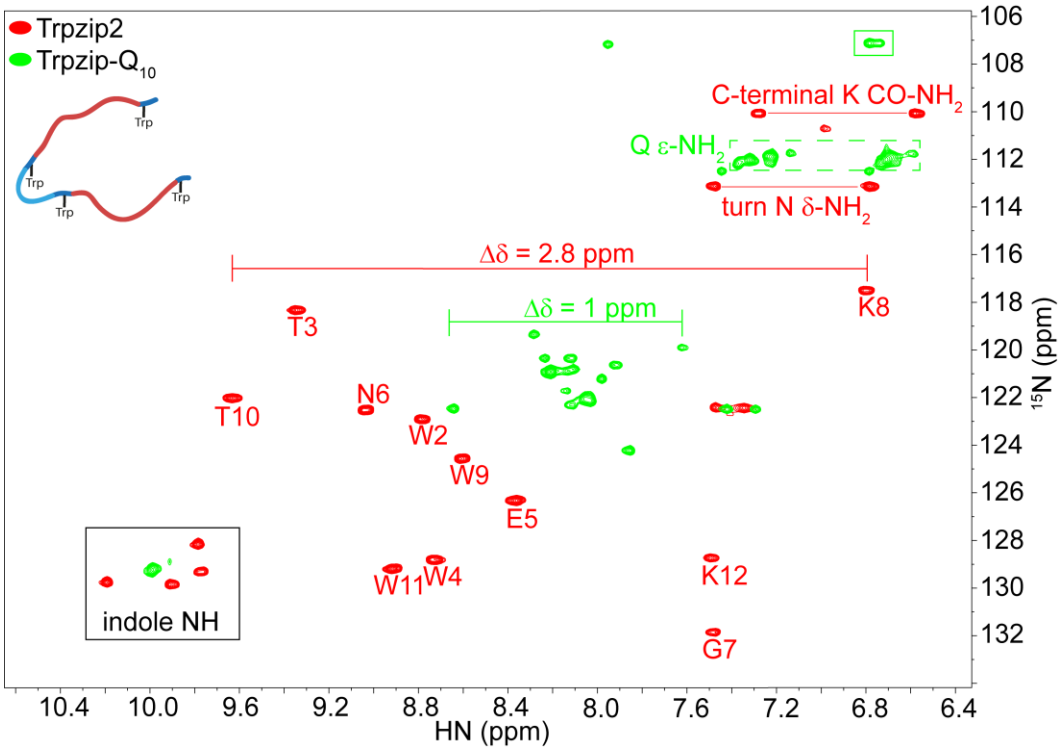

Figure S1c: Two-dimensional ^{1}H-^{15}N-HSQC spectra of Trpzip-Q_{10} (green) at c = 1 mM (c = 2.7 mg mL^{-1}) and the template Trpzip2 (red) at c = 1.4 mM (c = 2.2 mg mL^{-1}). The dispersion of chemical shifts, $\Delta\delta$, observed for backbone amide protons of Trpzip-Q_{10} ($\Delta\delta$ = 1 ppm) is about a third of Trpzip2 ($\Delta\delta$ = 2.8 ppm), indicating strong structural changes of the peptide fold. A strong loss in Trp-Trp cross-strand interactions is indicated by the resonance signals of the indole protons (black frame): only two signals are resolved (green) suggesting a signal overlay of three indole protons. In contrast to Trpzip2 with four dispersed signals (red) caused by the tryptophan side chains with edge-to-face orientations, the indole protons of Trpzip-Q_{10} have similar chemical environments, thus no well-defined orientations of the tryptophan side chains anymore. Both peptides show dispersed signals for N δ-NH_2 of the asparagine in the turn, but drastic changes in the C-terminal lysine of Trpzip-Q_{10} are observed as an overlaid signal (green frame). Additionally, Trpzip-Q_{10} reveals signals of the glutamine side chains Q ε-NH_2 which overlap more strongly than in Trpzip-Q_6 (dashed green frame). We interpret the strong glutamine-induced conformational change of the backbone, the more disordered C-terminus and the loss of tryptophan side-chain orientations in such a way that Trpzip-Q_{10} adopts a predominantly disordered structure with only weak hairpin features remaining from Trp-Trp interactions and the turn-promoting Asn-Gly motif in the sequence. The glutamine repeats of 5 glutamines per strand show the same chemical environments for most of the side chains indicating flexible glutamine regions.

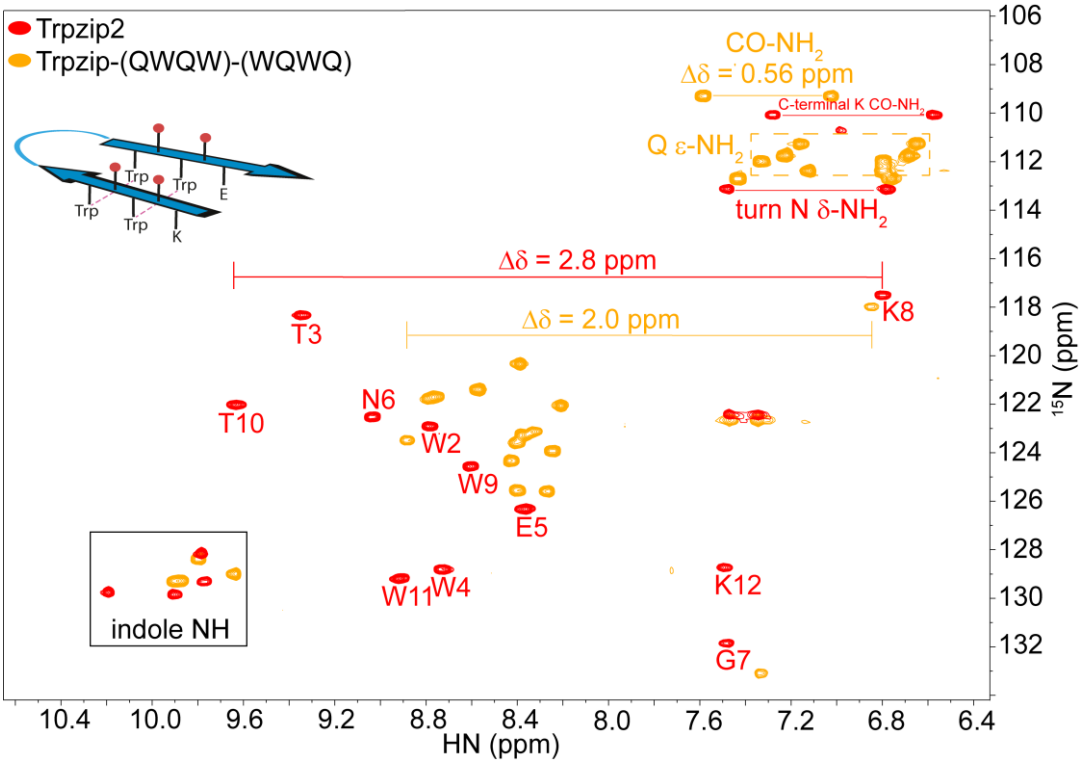

Figure S1d: Two dimensional ^{1}H-^{15}N-HSQC spectra of Trpzip-(QWQW)-(WQWQ) (orange) at c = 0.6 mM (c = 1.4 mg mL^{-1}) and the template Trpzip2 (red) at c = 1.4 mM (c = 2.2 mg mL^{-1}). The dispersion of chemical shifts, $\Delta\delta$, observed for backbone amide protons of Trpzip-(QWQW)-(WQWQ) is $\Delta\delta$ = 2 ppm, thus still relatively broad indicating only a moderate change of the template hairpin structure. This might result from the "tryptophan templating" (QWQW) of this peptide design which aims to imitate the hairpin stabilizing tryptophan frame of Trpzip2. However, the tryptophan indole NHs of Trpzip-(QWQW)-(WQWQ) show 4 less dispersed signals (with 2 overlapping) (black frame) similar to Trpzip-Q_6 (Fig. S1b). The C-terminal lysine carboxamide ($CO\text{-}NH_2$) and the turn asparagine side-chain amide N $\delta\text{-}NH_2$ both show two pairs of well dispersed cross signals similar to Trpzip2. Strikingly, the four amides of the glutamine side chains Q $\varepsilon\text{-}NH_2$ (highlighted using an orange frame, dashed mode) exhibit four pairs of well dispersed NH signals which indicate individual chemical environment of the glutamine side chains. We interpret the data in that way that Trpzip-(QWQW)-(WQWQ) adopts a hairpin structure and the "tryptophan templating" provides a structured environment for the glutamine side chains.

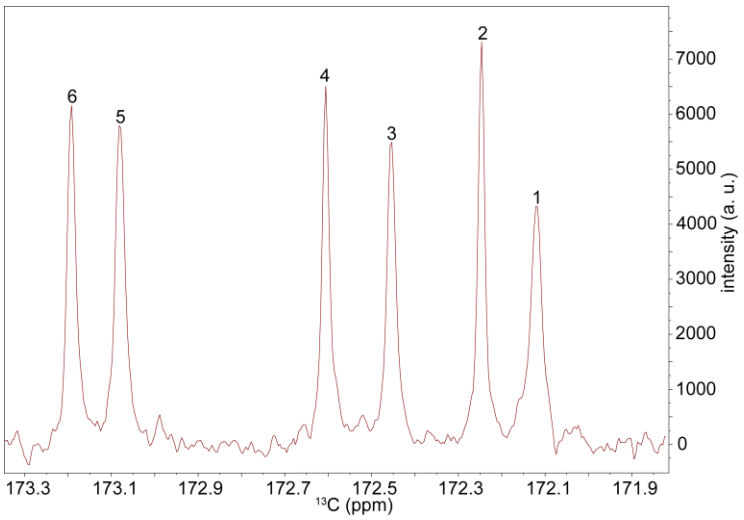

Figure S2a: One-dimensional ^{13}C NMR spectrum acquired for ^{13}C isotopically labeled Trpzip-Q_6 (AWQ*Q*Q*WENGKWQ*Q*Q*WK-NH_2). The backbone carbonyls of all six glutamines were isotopically labeled (^{13}C=O). Compared to Trpzip-Q_6, this peptide variant has a Ser-Ala substitution at the N-terminus, but we expect only a marginal impact on the backbone conformation of glutamine tracts, if any. This spectrum solely reveals the backbone conformation of inserted glutamines and shows six well separated resonance signals indicating a different chemical environment for each backbone carbonyl within the polyQ repeat of 3 glutamines per strand. This data is not contrary to the 2D ^{1}H-^{15}N HSQC spectrum (Fig. S1b) allowing conclusions about changes in the global fold of Trpzip-Q_6 (distorted hairpin), and not specifically about the conformation of the glutamine tracts. It is also not contrary to the finding that some of the glutamine side chains show similar chemical environments (Fig. S1b) due to solvent exposure promoting high inherent flexibility. Thus, we conclude that the backbone of the glutamines is constrained and forms a quite ordered strand. The concentration of Trpzip-Q_6 has been set to c = 0.7 mM (c = 1.5 mg mL^{-1}) and experimental data have been measured at T = 298 K.

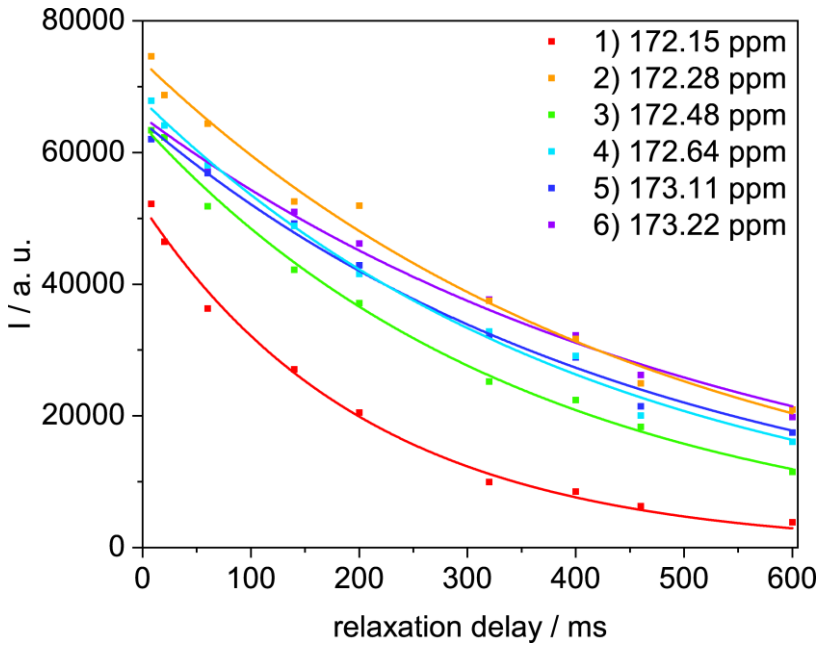

Figure S2b: Determination of the transverse relaxation time T_2 (Table S1) of isotopically labeled 1-^{13}C Trpzip-Q_6 at a residue-by-residue basis using a mono-exponential function (continuous line; fitting results are presented in Table S1). The labeling of signals has been done according to Fig. S2a.

Table S1: Transversal relaxation times obtained for Trpzip-Q_6 acquired at T = 298 K. Four ^{13}C labeled backbone carbonyl resonances of the glutamines show different (#1, #3, #4, #6), and two (#2, #5) show similar transversal relaxation times T_2**.** Although we did not assign the glutamines in the sequence we propose that the two similar relaxation times might be caused by the cross-strand glutamine pair in the middle of the glutamine repeats (Q4-Q13) with similar local environments.

Group chemical shift [ppm]	***T*₂ relaxation time [ms][a]**
1) 172.15	210 ± 10
2) 172.28	470 ± 20
3) 172.48	360 ± 10
4) 172.64	420 ± 20
5) 173.11	460 ± 20
6) 173.22	540 ± 20

[a] Errors are obtained from the applied fit function.

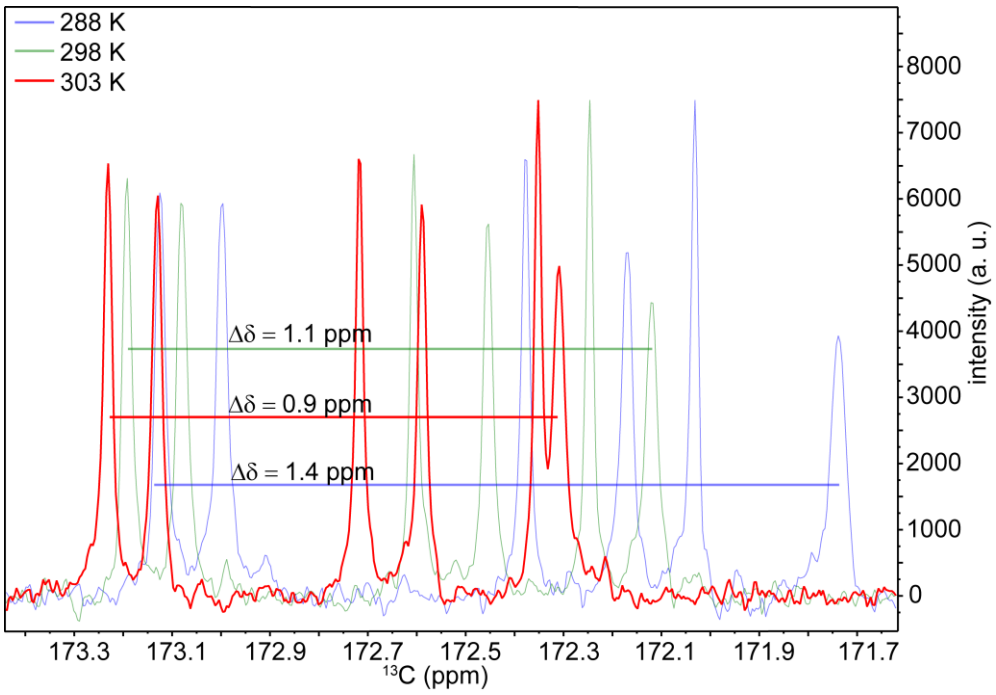

Figure S2c: Temperature-dependent one-dimensional ^{13}C NMR spectra of isotopically 1-^{13}C labeled glutamines of Trpzip-Q_6 (AWQ*Q*Q*WENGKWQ*Q*Q*WK-NH_2) acquired at different temperatures: T = 288 K (blue line), T = 298 K (green line) and T = 303 K (red line). The dispersion of the six resonance signals at T = 288 K is $\Delta\delta$ = 1.4 ppm, at T = 298 K the dispersion decreases to $\Delta\delta$ = 1.1 ppm and at T = 303 K to $\Delta\delta$ = 0.9 ppm. The decrease of the dispersion of chemical shifts at higher temperatures indicates a structural change of the polyQ repeat to a more unstructured peptide backbone.

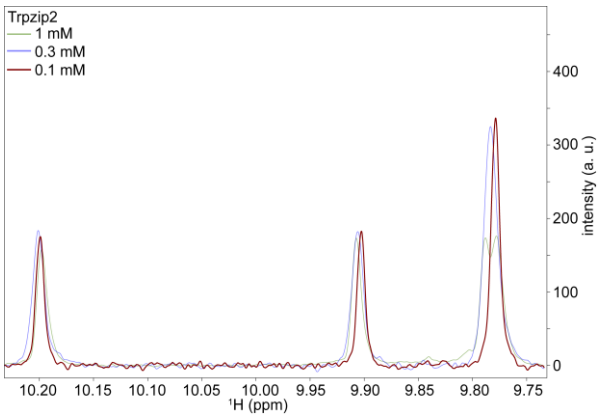

Figure S3a: One-dimensional ^{1}H NMR spectra of Trpzip2 at different concentrations: *c* = 1 mM (green), *c* = 0.3 mM (blue) and *c* = 0.1 mM (red). Upon a 10 fold dilution from *c* = 1 mM to *c* = 0.1 mM, only small changes in chemical shifts are observed in the indole region ($\Delta\boldsymbol{\delta} \leq \mathbf{0.01}\ \boldsymbol{ppm}$) and in the region of the amide backbone protons ($\Delta\boldsymbol{\delta} \leq \mathbf{0.043}\ \boldsymbol{ppm}$; 6.4 ppm - 9.7 ppm; data not shown). Line widths of resonance signals are conserved, too.

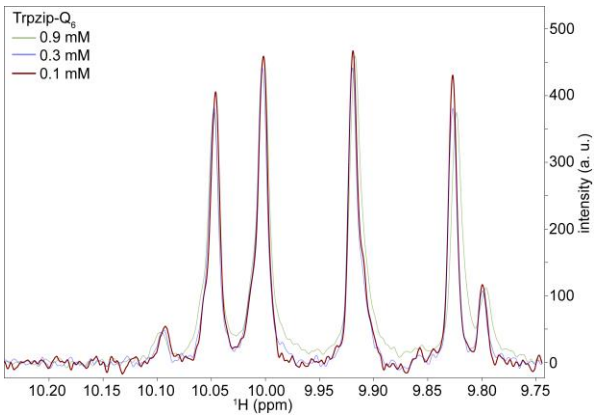

Figure S3b: One-dimensional ^{1}H NMR spectra of Trpzip-Q_6 focusing on the indole signal region acquired at different concentrations: *c* = 0.9 mM (green), *c* = 0.3 mM (blue), and *c* = 0.1 mM (red). Extremely small changes in chemical shift, $\Delta\boldsymbol{\delta} \leq \mathbf{0.0035}\ \boldsymbol{ppm}$, are observed upon dilution indicating no structural effect on the indole groups. Line widths of resonance signals are conserved, too. The changes in the amide backbone $\Delta\boldsymbol{\delta} \leq \mathbf{0.023}\ \boldsymbol{ppm}$ are also minor (data not shown).

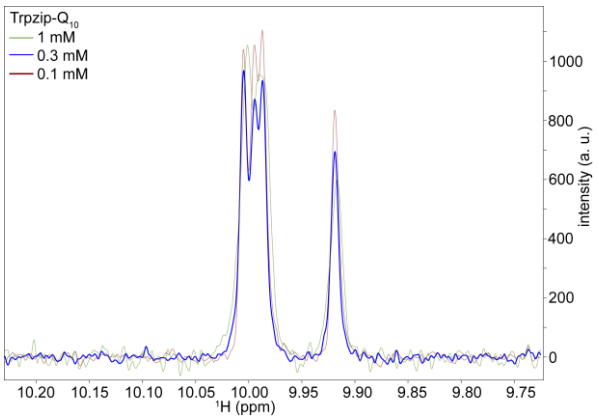

Figure S3c: One-dimensional ^{1}H NMR spectra acquired for Trpzip-Q_{10} at different concentrations of *c* = 0.9 mM (green), *c* = 0.3 mM (blue) and *c* = 0.1 mM (red) representing the indole region of chemical shifts. Extremely small changes in chemical shifts, $\Delta\boldsymbol{\delta} \leq \mathbf{0.003}\ \boldsymbol{ppm}$, are observed upon dilution indicating no structural impact on the indole groups comprising tryptophan residues. Increasing the concentration of Trpzip-Q_{10} goes along with a slight increase in line width of resonance signals indicating apparent slower tumbling of Trpzip-Q_{10}. The changes in the amide backbone $\Delta\boldsymbol{\delta} \leq \mathbf{0.01}\ \boldsymbol{ppm}$ are also minor (data not shown).

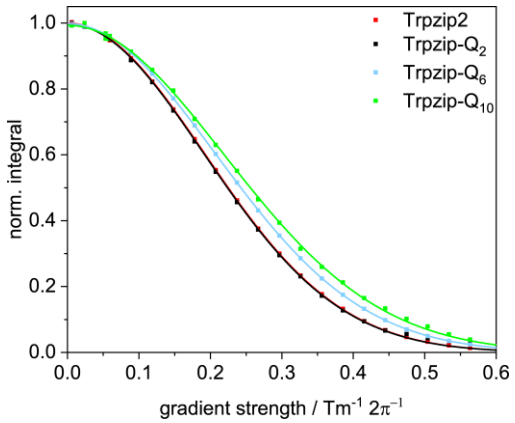

Figure S4: Pulse-field gradient NMR diffusion experiments of Trpzip2 (red), Trpzip-Q_2 (black), Trpzip-Q_6 (blue) and Trpzip-Q_{10} (green). The squares represent values of normalized integrals from the experimental ^{1}H spectra of the aliphatic signals between 0.5 and 4 ppm. The data was fitted according to (eq. 1, main text) to determine the diffusion coefficient. The concentration of the samples was about 1-2 mM, T = 298 K. Different compounds in solution are resolved based on their different diffusion coefficients, which depend on the size and shape of the molecule, thus the loss of monomeric structures and aggregation events become detectable.

Table S2: Data derived from diffusion NMR experiments. *N*: Number of amino acids; *D*: diffusion coefficient; r_h: hydrodynamic radius; $r_h^{th,monomer/dimer}$: hydrodynamic radius theoretically expected for a monomeric/dimeric properly folded peptide of this length. The size of the peptide was determined by calculating the hydrodynamic radius (eq. 2, main text) from the measured diffusion coefficient D (eq. 1, main text) and compared to a theoretical hydrodynamic radius of a polypeptide chain (eq. 3, main text) comprising the same number of amino acids. [1] Trpzip2 and Trpzip-Q_2 have similar hydrodynamic radii which match very well the theoretical values confirming the monomeric states. The diffusion coefficients for Trpzip-Q_6 and Trpzip-Q_{10} become smaller as expected because of the larger molecule size. Comparing the experimental and theoretical hydrodynamic radii for a monomer, the experimental values are about 10 % larger, but clearly exclude oligomerization of Trpzip-Q_6 and Trpzip-Q_{10} since their hydrodynamic radii are also significant smaller than for a dimer in solution.

Peptide	***N***	***D* [m^2 s^{-1}] 10^{-10}**	**r_h [Å]**	**$r_h^{th,monomer}$ [Å]**	**$r_h^{th,\ dimer}$ [Å]**
Trpzip2	12	2.26 ± 0.01	9.66	9.76	11.94
Trpzip-Q_2	12	2.27 ± 0.01	9.61	9.76	11.94
Trpzip-Q_6	16	1.93 ± 0.01	11.31	10.61	12.98
Trpzip-Q_{10}	20	1.73 ± 0.01	12.62	11.32	13.84

CD data

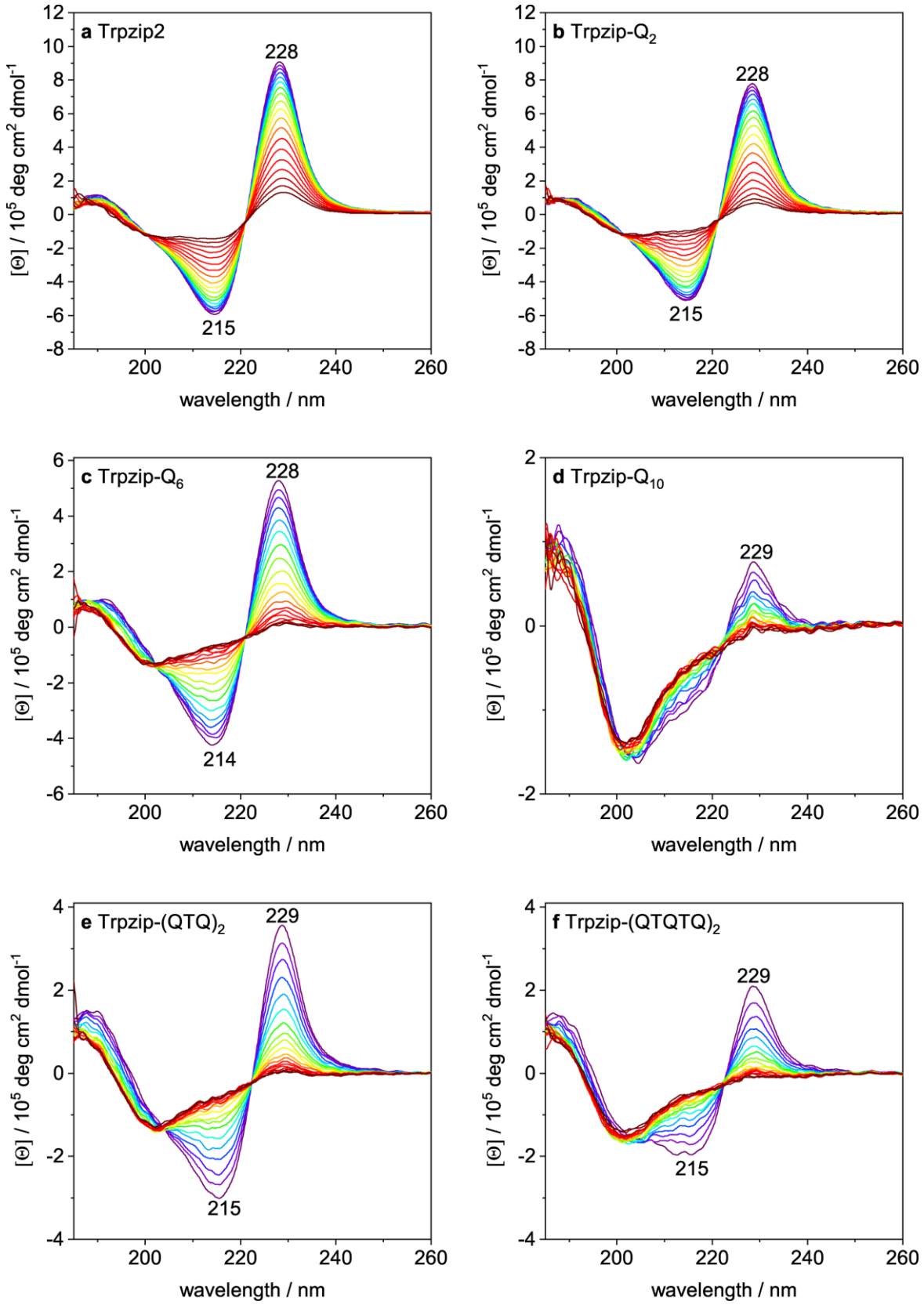
a Trpzip2
228
215
b Trpzip-Q2
228
215
c Trpzip-Q6
228
214
d Trpzip-Q10
229
e Trpzip-(QTQ)2
229
215
f Trpzip-(QTQTQ)2
229
215
[Θ] / 10^5 deg cm^2 dmol^-1
wavelength / nm

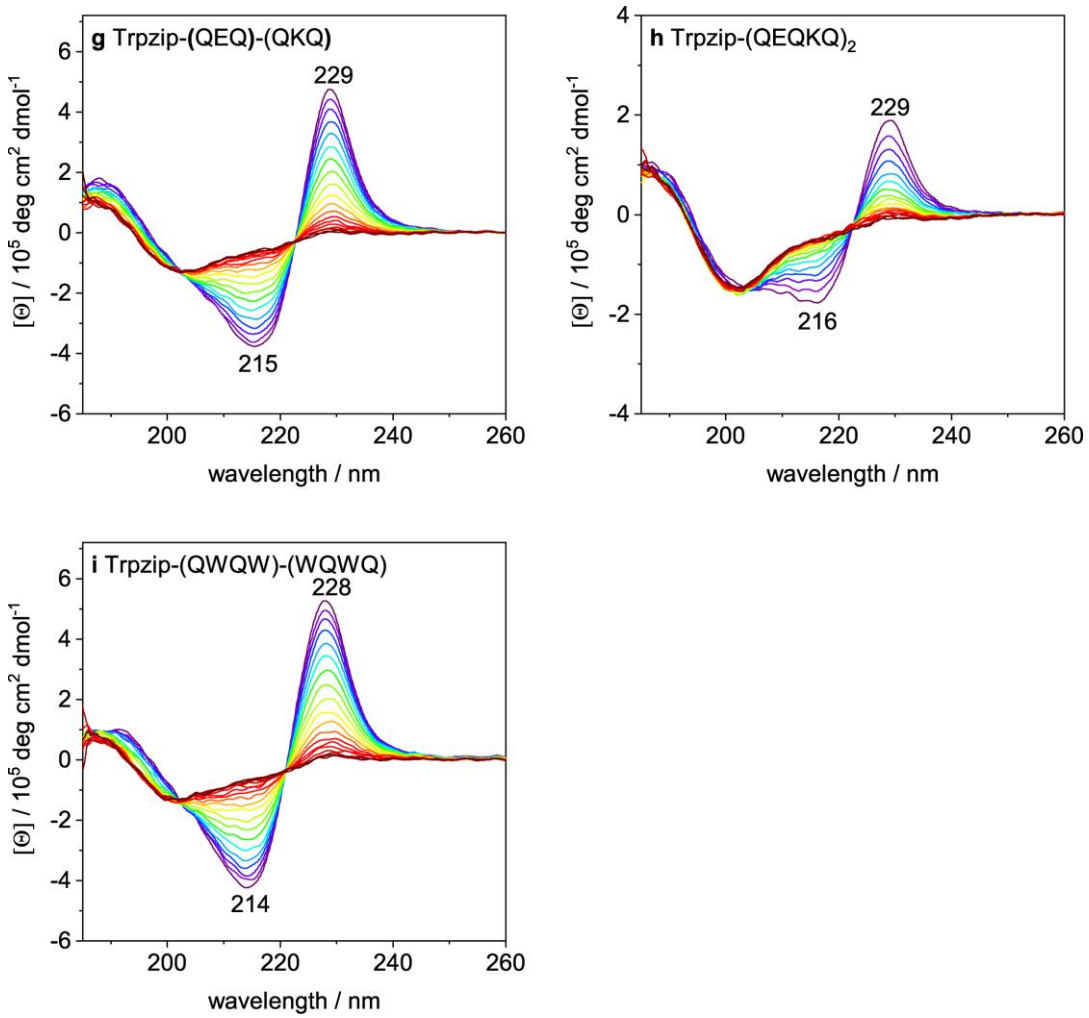

Figure S5: Temperature-dependent CD spectra acquired for **a** Trpzip2, **b** Trpzip-Q_2, **c** Trpzip-Q_6, **d** Trpzip-Q_{10}, **e** Trpzip-$(QTQ)_2$, **f** Trpzip-$(QTQTQ)_2$, **g** Trpzip-(QEQ)-(QKQ), **h** Trpzip-$(QEQKQ)_2$ and **i** Trpzip-(QWQW)-(WQWQ) in the temperature range from 5 °C (blue colourish) to 95 °C (red colourish). The Trp-Trp cross-strand pairs exhibit a negative signal at ~215 nm and a positive signal at ~228 nm. At a higher temperature, the Trp-Trp interactions are reduced due to the unfolding of the hairpin structure. Trpzip-Q_{10} shows almost no Trp-Trp interactions indicating a more disordered peptide with only minor hairpin features. Concentrations of peptides were ~ 0.1 mg mL^{-1}.

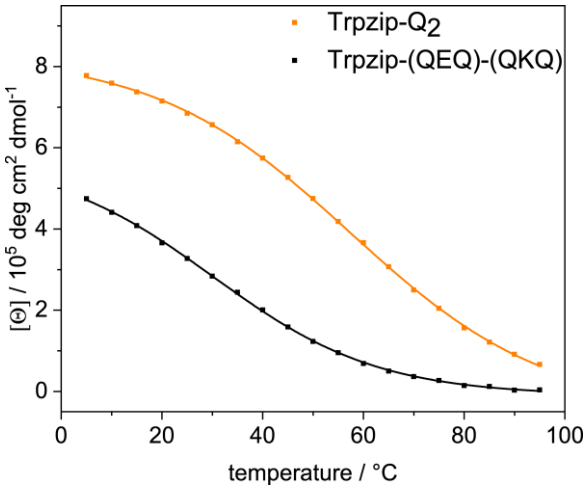

Figure S6: Sigmoidal fits of the transition curves of Trpzip-Q_2 and Trpzip-(QEQ)-(QKQ) obtained from the intensity change at ~228 nm from temperature-dependent CD spectra (5-95 °C). Fitting results using equation (eq. S2) are presented in Table S4. Concentrations of peptides were ~ 0.1 mg mL^{-1}.

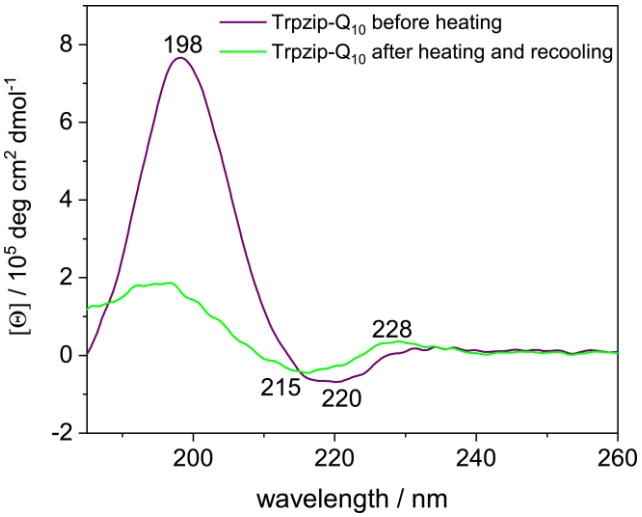

Figure S7: CD spectra acquired for Trpzip-Q_{10} showing β-sheet structure at 20 °C (colored in magenta), indicated by the band at 198 nm, which disappears upon heating to 90 °C and subsequent recooling (colored in green). The weak intensities of the bands at 228 nm and 215 nm indicate almost no exciton coupling of Trp residues. Concentration of the peptide was ~ 0.1 mg mL^{-1}.

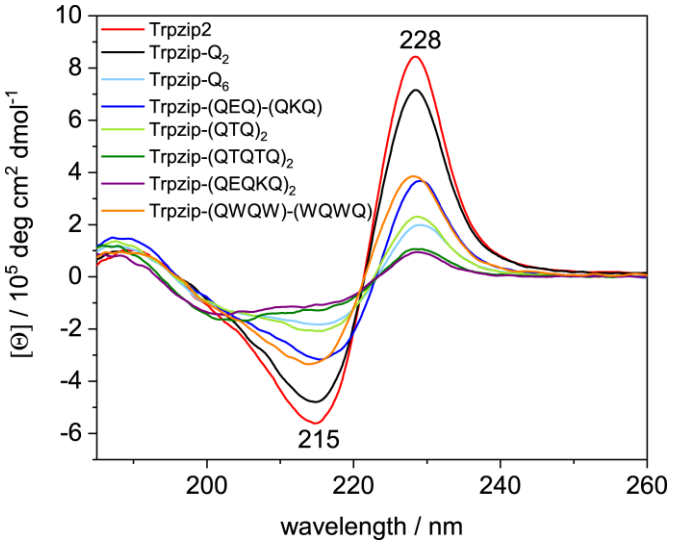

Figure S8: Comparison of CD spectra acquired for Trpzip2, Trpzip-Q_2, Trpzip-Q_6, Trpzip-$(QXQ)_2$, Trpzip-(QXQ)-(QYQ) and Trpzip-(QWQW)-(WQWQ) peptides at 20 °C. The intensity of the exciton bands at 228 nm and 215 nm decreases for Trpzip-(QEQ)-(QKQ), Trpzip-$(QTQ)_2$ and Trpzip-Q_6 indicating less Trp-Trp cross-strand interactions. Trpzip-(QEQ)-(QKQ) has a higher intensity of the band at 228 nm in comparison to the other two variants. Trpzip-(QWQW)-(WQWQ) is comparable to Trpzip-(QEQ)-(QKQ). Trpzip-$(QTQTQ)_2$ and Trpzip-$(QEQKQ)_2$ reveal the lowest intensity of the bands at 228 nm and 215 nm, indicating almost no Trp-Trp cross-strand interactions. The peptides were measured at similar concentrations of ~ 0.1 mg mL^{-1}.

IR data

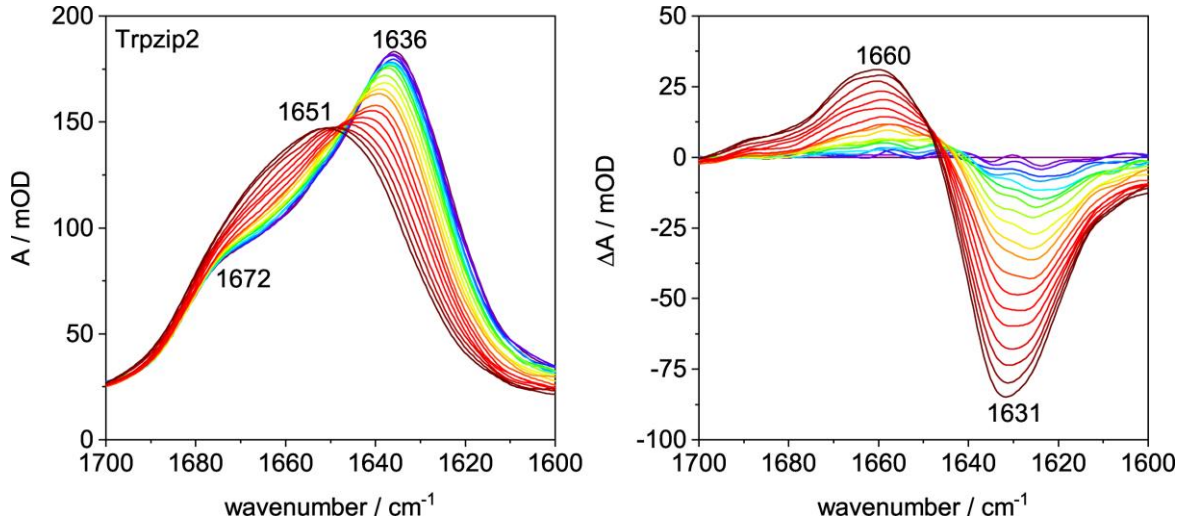

Figure S9: FTIR absorption spectra (left) and the corresponding difference spectra (right) of the template Trpzip2 (c = 10 mg mL^{-1}) in the amide I' region. Spectra were measured in the temperature range from 5 °C (blue colourish) to 95 °C (red colourish) in steps of 5 °C. At low temperatures Trpzip2 adopts an antiparallel monomeric β-hairpin which is shown by the bands at 1636 cm^{-1} and 1672 cm^{-1}. The disordered structure is indicated by the band shift to 1651 cm^{-1}. The peptide could reversibly be un- and refolded. Difference spectra are referenced to the 5 °C spectrum and reveal the wavenumbers with the maximum absorbance changes upon heating.

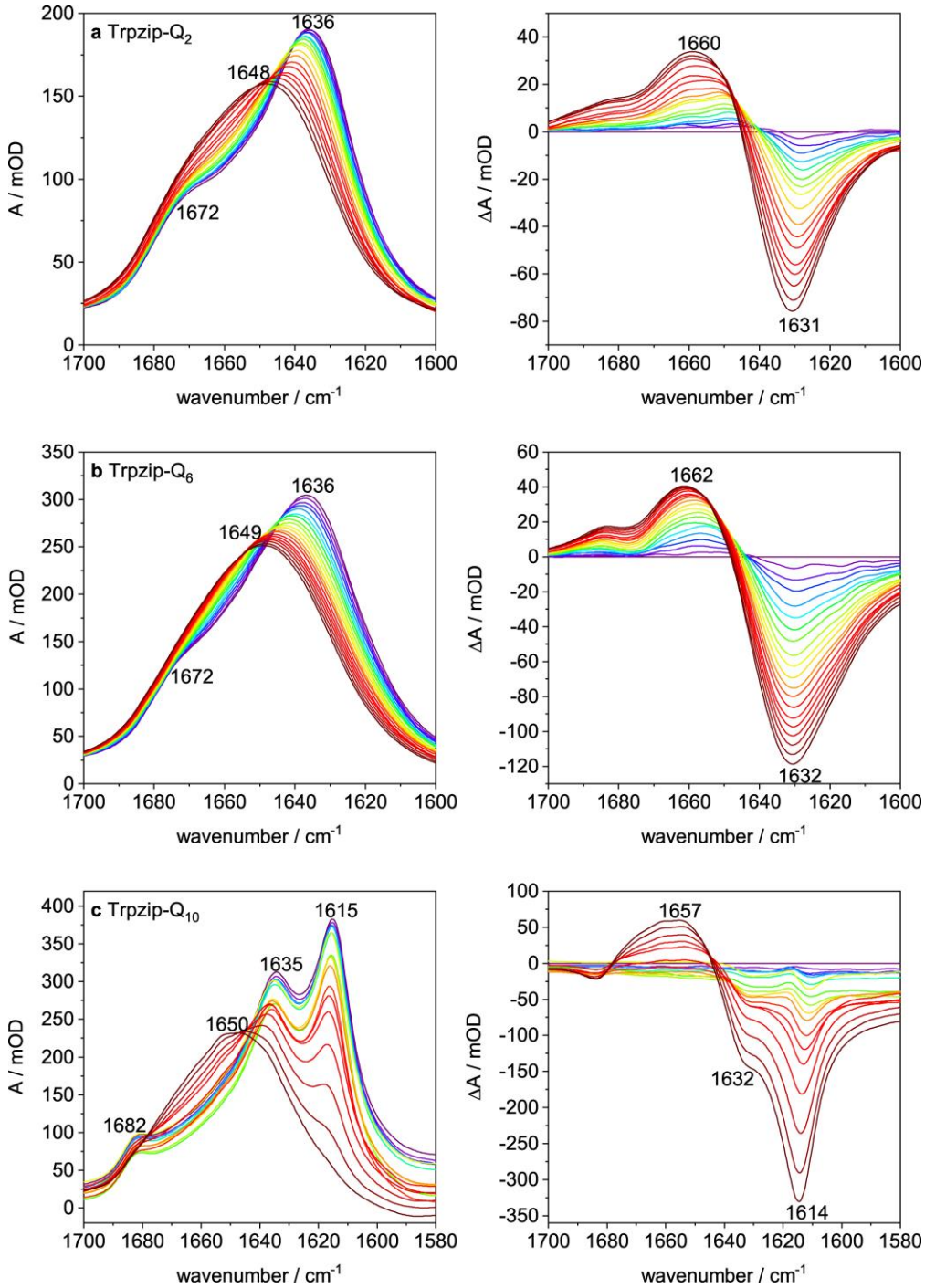

Figure S10: FTIR absorption spectra (left) and the corresponding difference spectra (right) of the design Trpzip-Q_n in the amide I' region **a** Trpzip-Q_2, **b** Trpzip-Q_6 and **c** Trpzip-Q_{10}. All peptides were measured at a concentration of 10 mg mL^{-1} and spectra were recorded in the temperature range from 5 °C (blue colourish) to 95 °C (red colourish) in steps of 5 °C. At low temperatures Trpzip-Q_2 and Trpzip-Q_6 reveal characteristic features of an antiparallel β-hairpin which is shown by the bands at 1636 cm^{-1} and 1672 cm^{-1}. The band at 1636 cm^{-1} also contains contributions from the glutamine carbonyl side-chain absorbance. At higher temperatures the band maximum shifts to higher wavenumber which indicates a loss of β-hairpin structure and the rise of disordered structure. Trpzip-Q_2 and Trpzip-Q_6 could be reversibly un- and refolded. Trpzip-Q_{10} forms an oligomeric β-sheet structure indicated by the bands at 1615 cm^{-1} and 1682 cm^{-1}. The band at 1635 cm^{-1} can be assigned to the glutamine side chains.

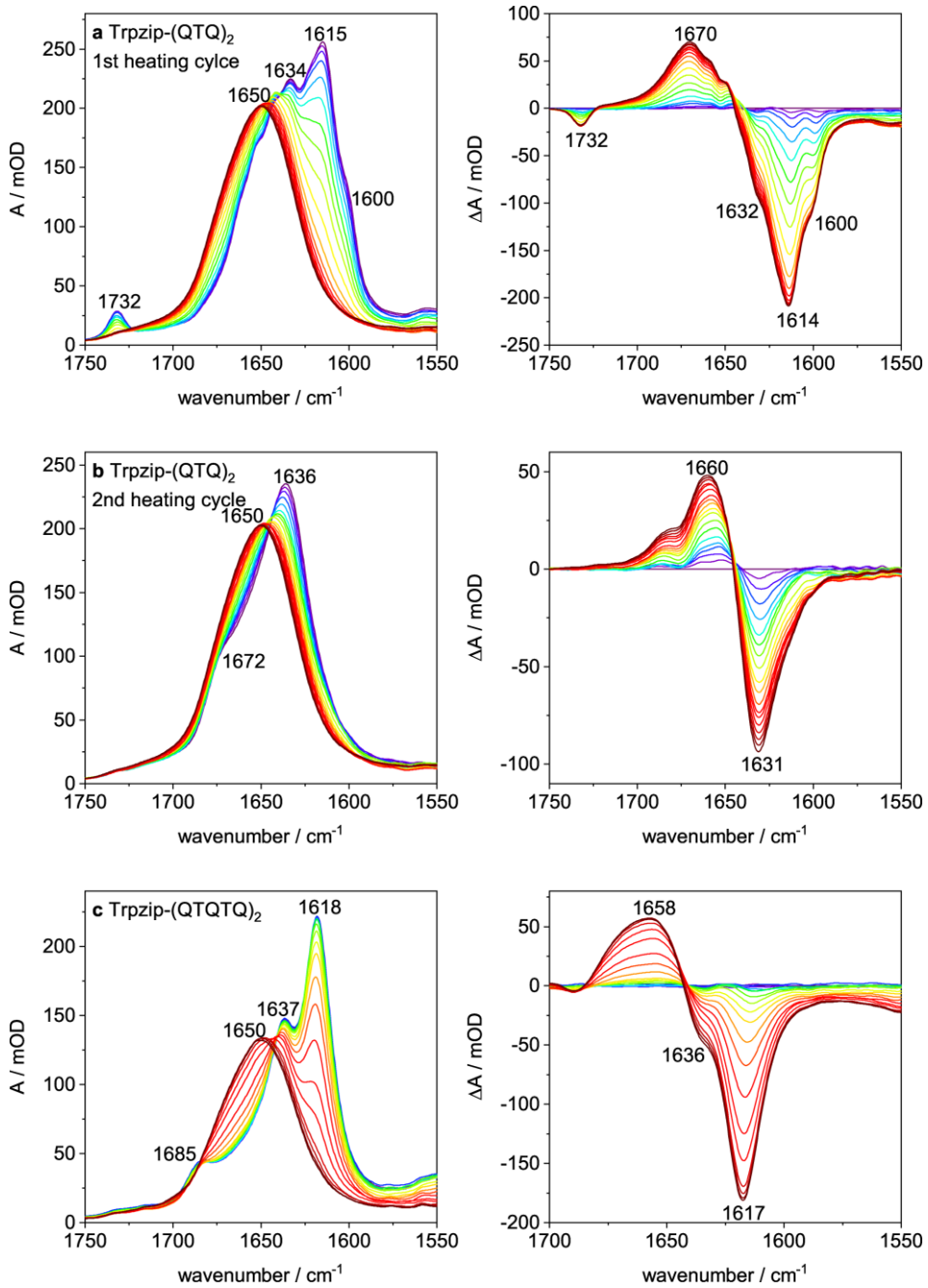

Figure S11: FTIR absorption spectra (left) and the corresponding difference spectra (right) of the design Trpzip-$(QXQ)_2$. **a** & **b** Trpzip-$(QTQ)_2$ and **c** Trpzip-$(QTQTQ)_2$ peptides in the amide I' region in the temperature range of 5 °C (blue colourish) and 95 °C (red colourish) measured in steps of 5 °C. All peptides were measured at a concentration of 10 mg mL^{-1}. **a** Trpzip-$(QTQ)_2$ forms an initial oligomeric sheet structure indicated by the band at 1615 cm^{-1} which can be converted into a disordered structure at high temperatures (first heating cycle). The band at 1732 cm^{-1} might occur from a protonated carboxylic side–chain group (glutamic acid) in the oligomeric state, however it was not observed for other peptide variants with oligomeric states. **b** A hairpin structure is formed after recooling which could be reversibly un- and refolded in the second heating cycle. The band at 1732 cm^{-1} disappears after disaggregation into a monomeric state. **c** Trpzip-$(QTQTQ)_2$ forms oligomeric sheet structures as shown by the bands at 1618 cm^{-1} and 1685 cm^{-1}. At high temperature, the peptide could be transferred into a disordered structure, but the oligomeric sheet structure is formed again (at the here studied concentration) after recooling similar to Trpzip-Q_{10}.

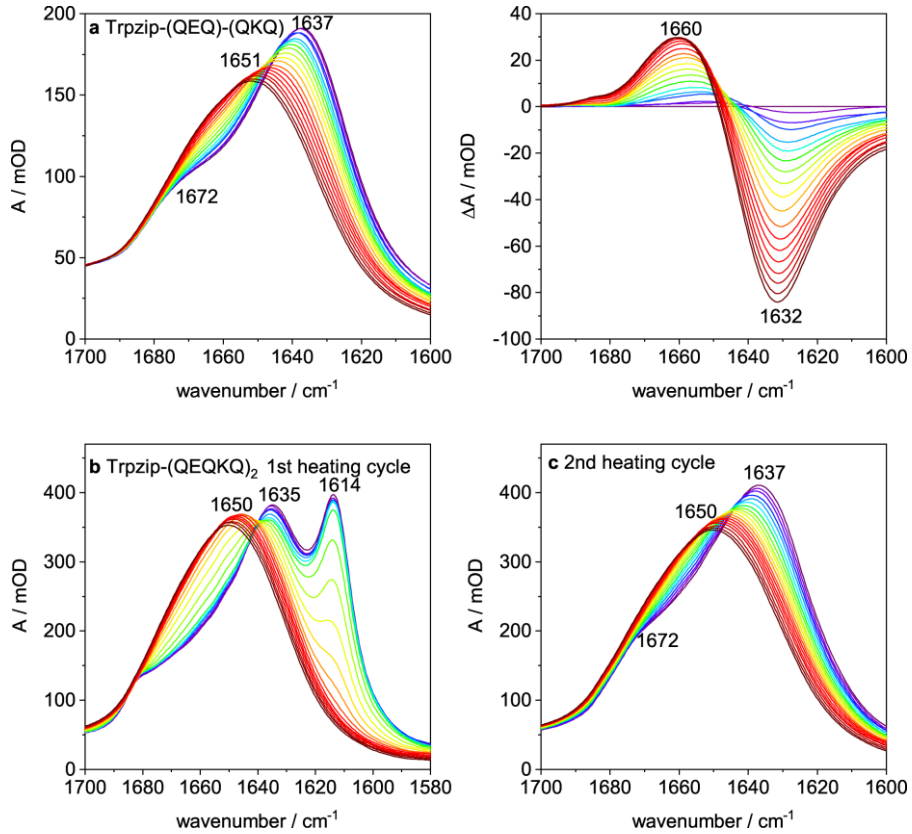

Figure S12: FTIR absorption spectra and corresponding difference spectra of the design Trpzip-(QXQ)(QYQ). **a** Trpzip-(QEQ)-(QKQ) and **b** & **c** Trpzip-(QEQKQ)$_2$ in the amide I' region in the temperature range of 5 °C (blue colourish) to 95 °C (red colourish) measured in steps of 5 °C. All peptides were measured at a concentration of 10 mg mL^{-1}. **a** Trpzip-(QEQ)-(QKQ) forms a hairpin structure indicated by the bands at 1637 cm^{-1} and 1672 cm^{-1}. The peptide could be reversibly unfolded and refolded. **b** Trpzip-(QEQKQ)$_2$ forms an initial oligomeric sheet structure indicated by the bands at 1614 cm^{-1} and 1682 cm^{-1}. **c** This variant can be transferred into a disordered structure upon heating. After recooling, a hairpin structure is formed, which could be reversibly un- and refolded.

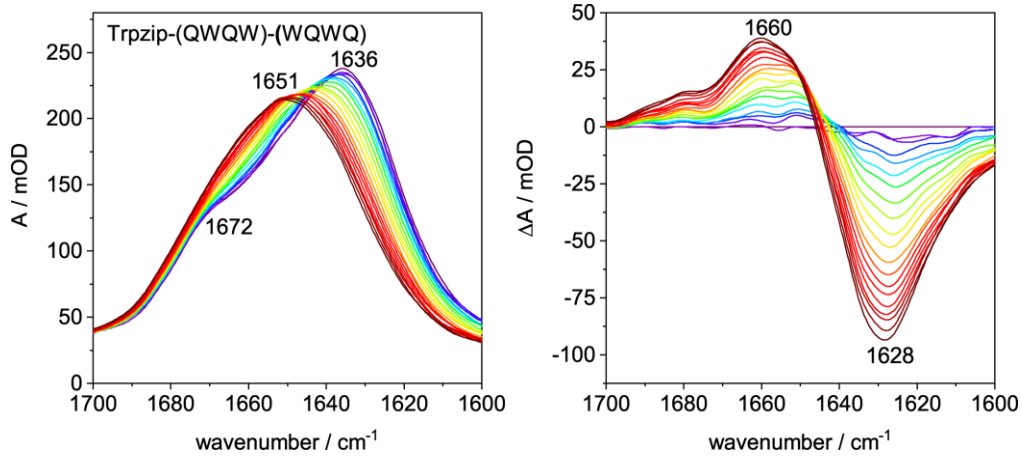

Figure S13: FTIR absorption (left) and corresponding difference spectra (right) of Trpzip-(QWQW)-(WQWQ) in the amide I' region measured in the temperature range of 5 °C (blue colourish) to 95 °C (red colourish) in steps of 5 °C and a concentration of 10 mg mL^{-1}. At low temperatures Trpzip-(QWQW)-(WQWQ) reveals characteristic features of an antiparallel β-hairpin which is shown by the bands at 1636 cm^{-1} and 1672 cm^{-1}. At higher temperatures the band maximum shifts to higher wavenumber which indicates the loss of β-hairpin structure and the rise of a disordered structure. Trpzip-(QWQW)-(WQWQ) could be reversibly un- and refolded.

Data analysis of temperature-dependent FTIR and CD spectra

Single value decomposition (SVD) of FTIR temperature-dependent spectra was performed using Matlab software, MA (USA). This method uses the following equation

$$D = USV^T \qquad (\mathrm{eq.S1})$$

The raw data matrix, D will be transformed according to equation (1). U is the matrix of basis set spectra that describes the data, V is the matrix of amplitude values as a function of experimental conditions (such as temperature) and S is the diagonal matrix containing singular values representing the contribution of basis spectra to the data set. The second component represents the largest spectral variation from the average and was used to perform the fits.

Transition temperatures for IR spectroscopic data were determined by the thermal analyses of the 2nd component of a singular value decomposition of the FTIR spectra (1700-1600 cm^{-1}).

Transition temperatures for CD spectroscopic data were obtained by fitting the intensity change of the band at ~228 nm of the CD spectra.

A Boltzmann function was used to fit the transitions with flat baselines and a sigmoidal shape.

$$y = \frac{A_1 - A_2}{1 + \exp((T - T_\mathrm{m})/\mathrm{d}t)} \qquad (\mathrm{eq.S2})$$

where A_1 is the initial value, A_2 the final value, d*t* the slope factor and T_m is the melting temperature.

However, the use of flat baselines for the folded and unfolded state is not always accurate. To overcome this problem an empirical approach based on a differential denaturation curve was used.[2] The temperature-dependent signals were algebraically differentiated. The data were evaluated with a two-state equilibrium model:

$$\frac{d(\mathrm{signal})}{\mathrm{d}T} = Af(1-f)(T^2) \qquad (\mathrm{eq.S3})$$

where *d*(signal)/d*T* is the algebraic derivative of the 2nd component, A is a scaling factor and *f* is the fraction of denatured peptide.

For a two-state transition, *f* is related to the melting temperature (T_m) and van't Hoff enthalpy (ΔH_vm) by the equilibrium constant (*K*) for a unimolecular reaction:

$$f = \frac{K}{K+1} \qquad (\mathrm{eq.S4})$$

$$K = \exp\left[\frac{\Delta H_\mathrm{vm}}{R}\left(\frac{1}{T_\mathrm{m}} - \frac{1}{T}\right)\right] \qquad (\mathrm{eq.S5})$$

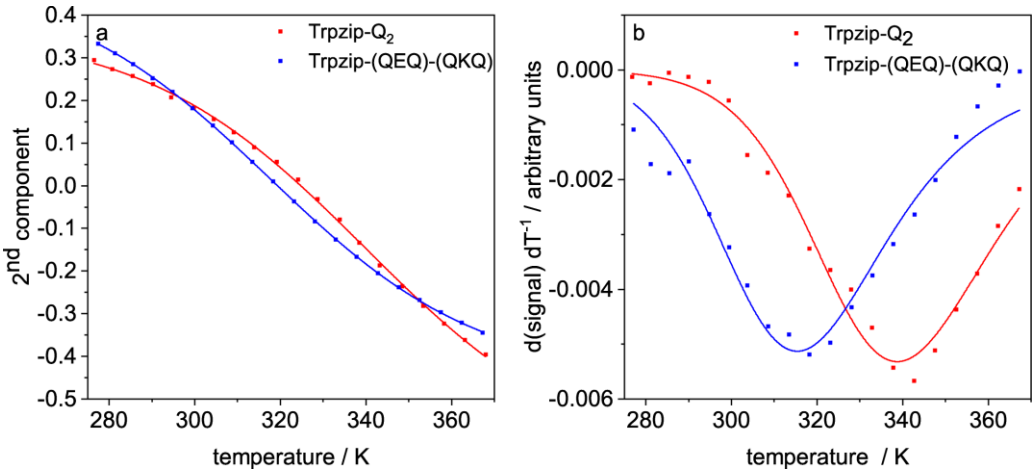

Figure S14: Comparison of the transition curves acquired for Trpzip-Q_2 and Trpzip-(QEQ)-(QKQ) applying SVD analysis in **a** and the algebraic derivatives of the 2nd components from the SVD analysis in **b**, data were fitted using a Boltzmann curve in **a** according to equation (eq. S2) and with a two state equilibrium model according to equation (eq. S3) in **b**.

Taking into account that the transition curves of Trpzip-Q_2 and Trpzip-(QEQ)-(QKQ) are broad, having different shapes and no flat baselines we tested an approach using the first algebraic derivative of the second component of SVD analysis to examine the difference of the transition temperature. We obtained slightly smaller transition temperatures for both variants but with the same trend as obtained by the SVD analysis (Table S3). This shows that the fitting procedure using the Boltzmann equation comprising flat baselines is suitable for analyzing thermodynamic features of polyQ peptides.

Table S3: Transition temperatures obtained for Trpzip-Q_2 and Trpzip-(QEQ)-(QKQ) determined by the thermal analyses of the 2nd component of a singular value decomposition of the FTIR spectra (1700-1600 cm^{-1}) with a concentration of 10 mg mL^{-1}. The transition temperatures obtained from the algebraically derivative of the 2nd component using eq. S2 are also shown (Fig. S13).

Peptide	**T_m [°C] SVD**	**T_m [°C][a] d(signal)/d*T***
Trpzip-Q_2	68 ± 1	64 ± 2
Trpzip-(QEQ)-(QKQ)	45 ± 3	40 ± 2

[a] T_m was mostly unaffected by y-axis translation which represents pre- and post-transitional baselines of the 2nd component. For a y-translation ± 0.001 arbitrary units T_m changed by ± 2 °C.

Table S4: Comparison of transition temperatures obtained from temperature-dependent FTIR and CD spectroscopic data acquired on polyQ-rich peptides. Transition temperatures for IR data were determined by the thermal analyses of the 2nd component of a singular value decomposition of the FTIR spectra (1700-1600 cm^{-1}) with a concentration of 10 mg mL^{-1} (Fig. S10-S13). Transition temperatures for CD data were obtained by fitting the intensity change of the bands at ~228 nm of the CD spectra (eq. S2) with a concentration of 0.1 mg mL^{-1}.

Peptides	T_m [°C][a] IR	T_m [°C][a] at ~228 nm CD
Trpzip-Q_2	68 ± 1	57 ± 1
Trpzip-Q_6	-[b]	-[b]
Trpzip-Q_{10}	78[c] ± 2	-[b]
Trpzip-$(QTQ)_2$	-[b]	-[b]
Trpzip-$(QTQTQ)_2$	65[c] ± 1	-[b]
Trpzip-(QEQ)-(QKQ)	45 ± 3	29 ± 1
Trpzip-$(QEQKQ)_2$	-[b]	-[b]
Trpzip-(QWQW)-(WQWQ)	39 ± 1	34 ± 1

[a] Errors of transition temperatures are determined from the standard deviation of repeated measurements.
[b] Transition curves are broad and have no clear sigmoidal shape, no reliable determination of transition temperatures was possible.
[c] Sample contains oligomeric sheet structures as indicated by the band at ~1615 cm^{-1} (Figs. S10c, S11c).

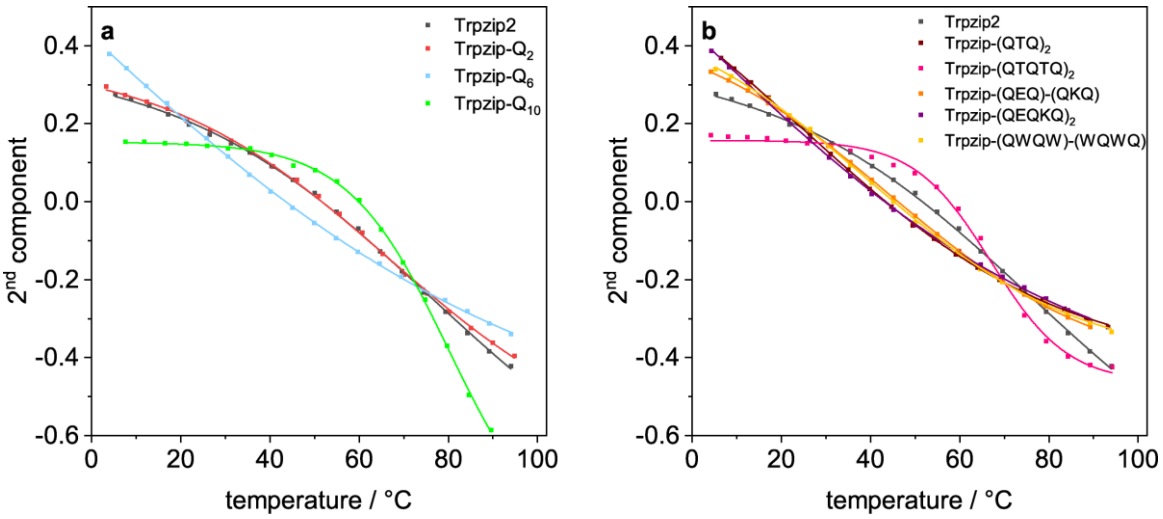

Figure S15: Comparison of the transition curves acquired for **a** Trpzip2 and Trpzip-Q_n models and **b** other designs applying SVD analysis. Data were fitted using a Boltzmann curve according to equation (eq. S2). The shape of the transition curves of Trpzip2 and Trpzip-Q_2 are sigmoidal and shows a cooperative character. As the glutamine content increases for Trpzip-Q_6, the transition curve becomes less cooperative and a lower transition temperature can be monitored. However, for Trpzip-Q_{10} the shape of the curve is more pronounced and a higher transition temperature is obtained due to the oligomeric character of this sequence. The same effects are observed for the other designs.

Disaggregation procedure of peptides

For some peptides, disaggregation of oligomeric structures can be achieved by heat treatment as shown exemplarily for Trpzip-$(QTQ)_2$ (Fig. S16a). An oligomeric structure is observed after dissolving the peptide in D_2O (1615 cm^{-1}). After heating (to ~70 – 80 °C for ~10 minutes) the oligomeric sheet structure is melted (data not shown), and the peptide refolds to a hairpin structure after recooling to ~17 °C, as indicated by the bands at 1637 cm^{-1} and 1672 cm^{-1}. Another strategy to overcome aggregation and to enhance the solubility is to substitute threonines with charged amino acids like lysine and glutamic acid. The exchange of threonines with lysine and glutamic acid in the peptide model (Trpzip-(QEQ)-(QKQ)) leads to β-hairpin monomers without heating (data not shown). The substitution of threonines in the peptide variant comprising elongated strands, Trpzip-$(QTQTQ)_2$, with one pair of lysine and glutamic acid in each strand leads to the variant Trpzip-$(QEQKQ)_2$ which also shows oligomerization (Fig. S16b). For this variant, precipitation was observed already during the lyophilization procedure. However, Trpzip-$(QEQKQ)_2$ can be transferred into a β-hairpin structure after heating and recooling. The FTIR measurements demonstrate how sensitively the elongation of the polyQ-rich sequence and the choice of charged amino acids influence the solubility respectively oligomerization of glutamine sequences, and furthermore that heating is a suitable tool for some of the variants to disaggregate initial oligomeric sheet structures and to transfer them into a monomeric state. It should be noted that the concentration is also crucial for aggregation behavior as outlined in our manuscript.

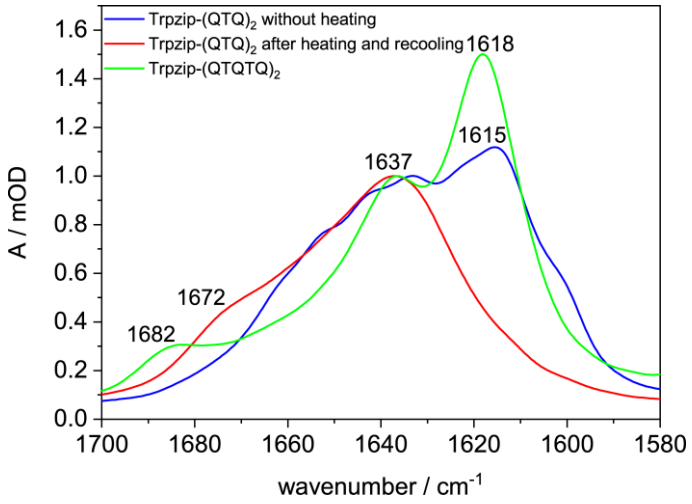

Figure S16a: Comparison of FTIR spectra (normalized to the intensity at 1637 cm^{-1}) acquired for Trpzip-$(QTQ)_2$ (colored in red, in blue) and Trpzip-$(QTQTQ)_2$ (colored in green) at ~17 °C and at a concentration of 10 mg mL^{-1}. In the Trpzip-$(QTQ)_2$ (blue line) oligomeric sheet structures are observed as indicated by the band at 1615 cm^{-1}. The oligomeric sheet structure can be unfolded upon heating (data not shown). After recooling, Trpzip-$(QTQ)_2$ forms a hairpin structure as indicated by the bands at 1637 cm^{-1} and 1672 cm^{-1} (red line). Elongation of the polyQ-rich strands to Trpzip-$(QTQTQ)_2$ (green line) leads to an oligomeric sheet structure (1618 cm^{-1} and 1682 cm^{-1}) similar as for Trpzip-Q_{10}. The oligomer cannot be transferred into a monomeric state by heat in this case.

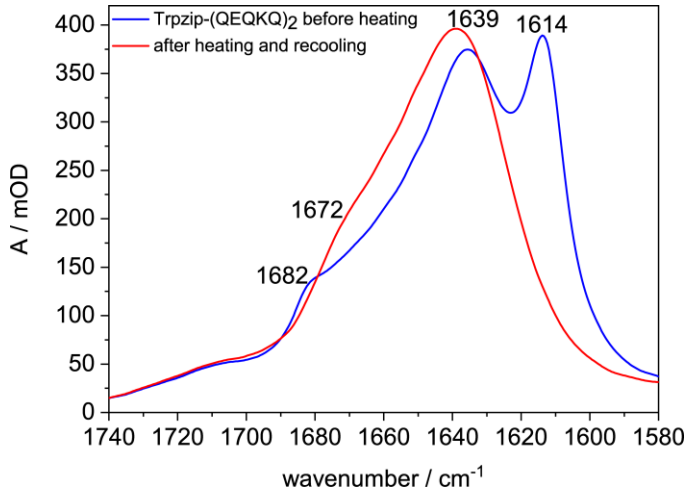

Figure S16b: Initial oligomeric sheet structure observed for Trpzip-$(QEQKQ)_2$ (blue line) before heating (1614 cm^{-1} and 1682 cm^{-1}) and its transition to a β-hairpin monomer after heating and recooling (1639 cm^{-1} and 1672 cm^{-1}). Spectra were recorded at ~17 °C and at a concentration of 10 mg mL^{-1}.

IR detected temperature-jump dynamics

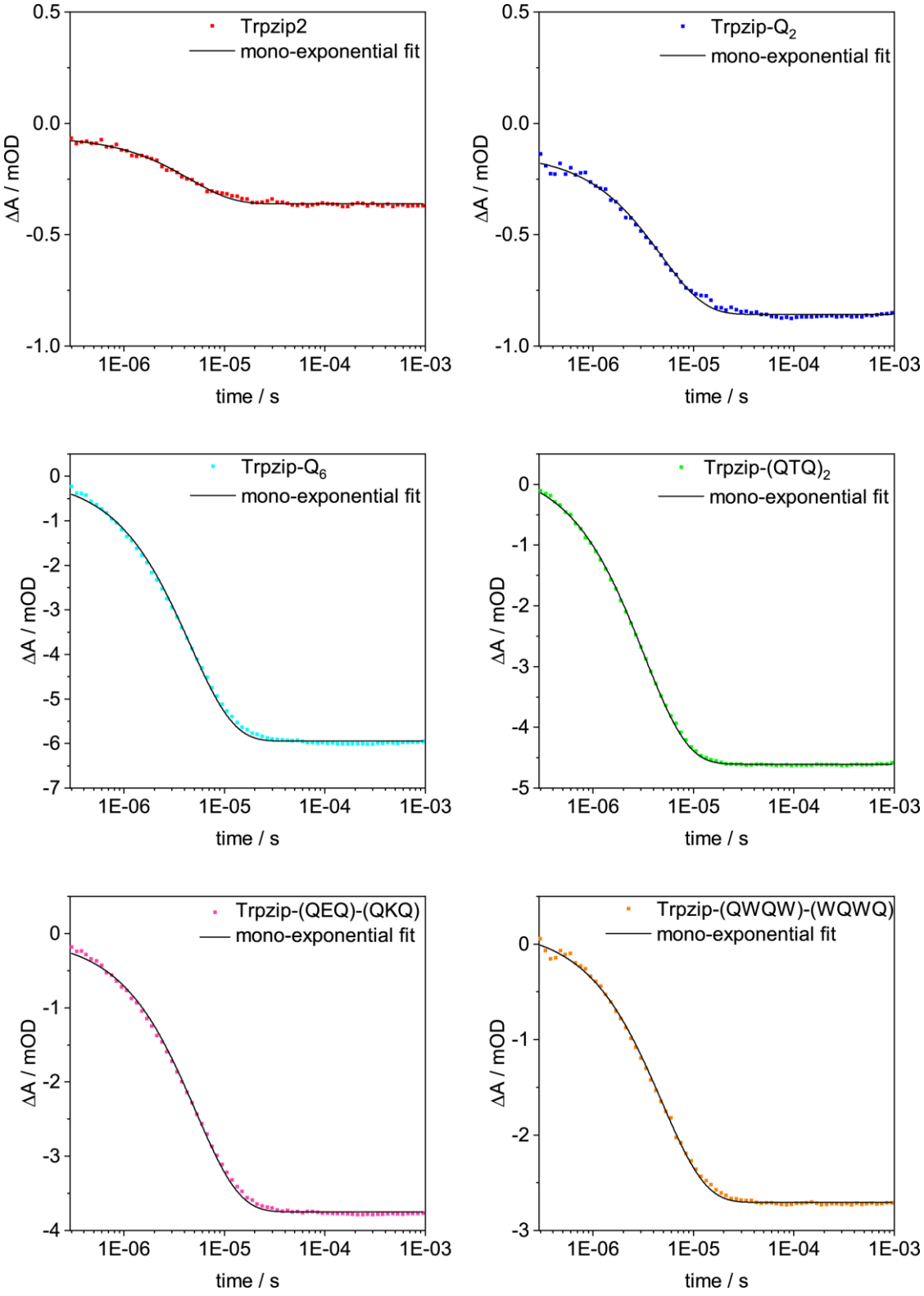

Figure S17: Solvent subtracted transients acquired for Trpzip2, Trpzip-Q_2, Trpzip-Q_6, Trpzip-$(QTQ)_2$, Trpzip-(QEQ)-(QKQ) and Trpzip-(QWQW)-(WQWQ) at ~1630 cm^{-1}, at a concentration of 10 mg mL^{-1} and a final temperature of ~25 °C after the T-jump. A mono-exponential fit was applied.

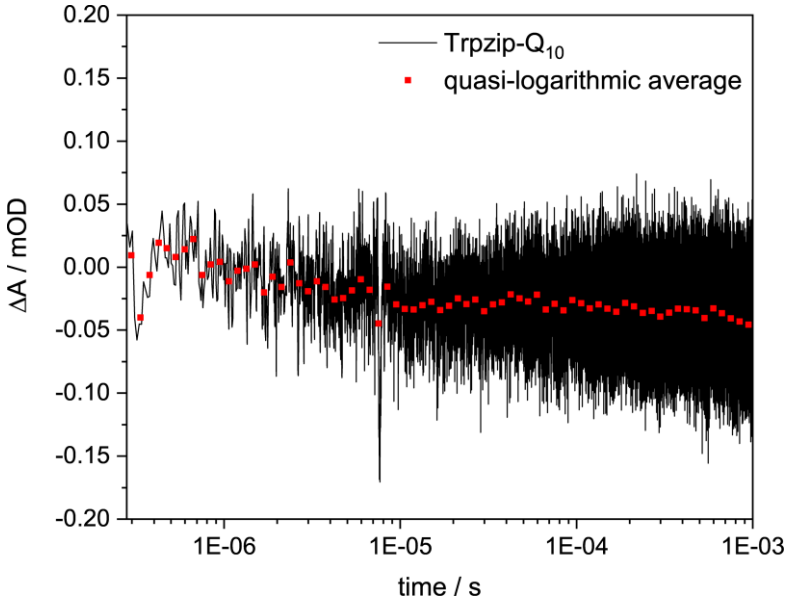

Figure S18a: A comparison of the solvent subtracted transient at 1632 cm^{-1} (raw data) and after a quasi-logarithmic averaging (red squares) with N = 20 points per decade shown for Trpzip-Q_{10}. The absorbance changes are too small and the data are not regarded as reliable for further processing.

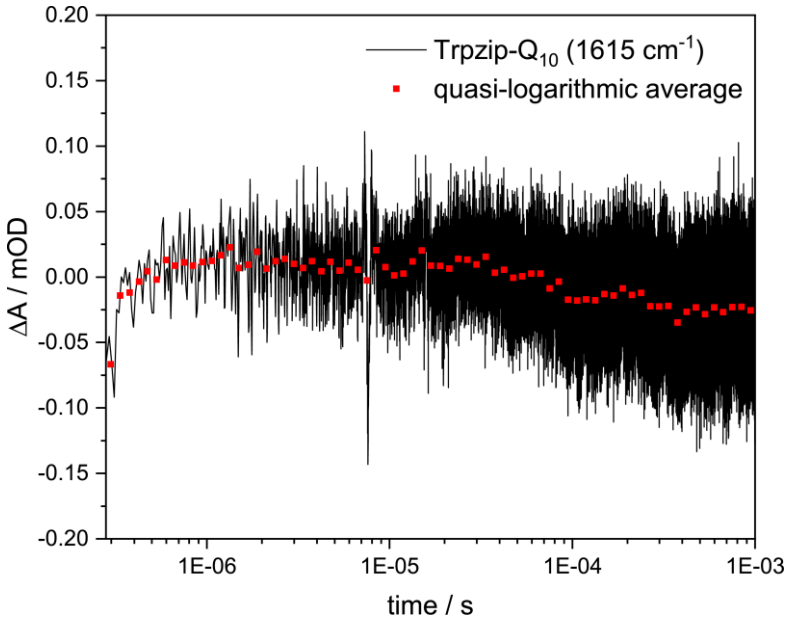

Figure S18b: A comparison of the solvent subtracted transient at 1615 cm^{-1} (raw data) and after a quasi-logarithmic averaging (red squares) with N = 20 points per decade for Trpzip-Q_{10}. The absorbance changes are too small under the measurement conditions used here and the data were not further analyzed.

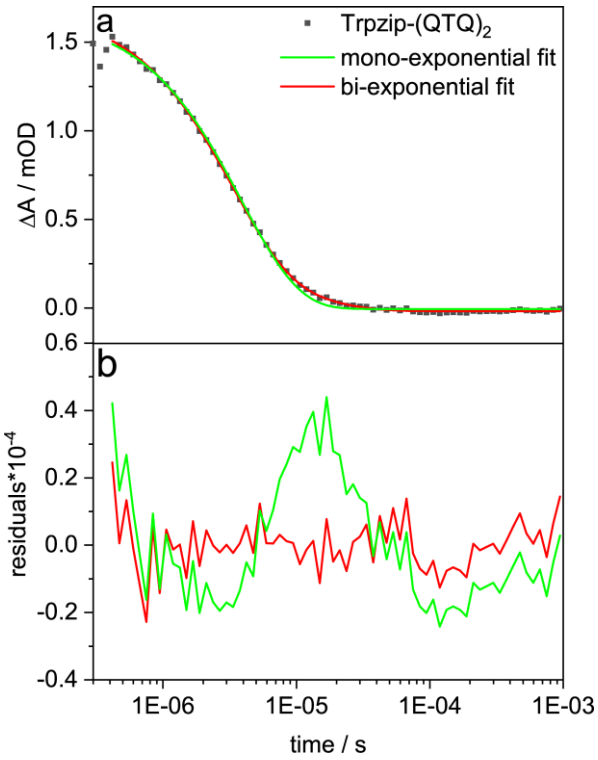

Figure S19a: a Transient determined for Trpzip-$(QTQ)_2$ at 1632 cm^{-1}, at a concentration of 10 mg mL^{-1} and a final temperature of ~25 °C after the T-jump. Mono- and bi-exponential fits are applied to the transient. **b** Residuals of the mono-exponential - and the bi-exponential fits are shown. The transient is not well described with a mono-exponential fit function and is better described using a bi-exponential fit.

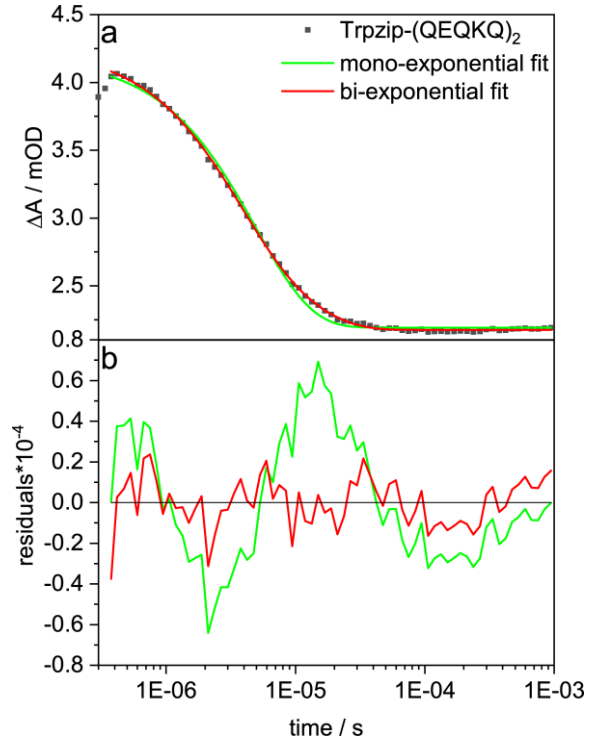

Figure S19b: a Transient determined for Trpzip-$(QEQKQ)_2$ at 1632 cm^{-1}, at a concentration of 10 mg mL^{-1} and a final temperature of ~25 °C after the T-jump. Mono- and bi-exponential fits are applied to the transient. **b** Residuals of the mono-exponential - and the bi-exponential fits are shown. The transient is better described using a bi-exponential fit.

Peptide characterization

Trpzip2

Certificate of analysis

peptides&elephants

www.peptides.de

Product	Pep2
Batch	0304Q02
ID	EP08327
Sequence	SWTWENGKWTWK-NH2
MW	1607.7

Purity

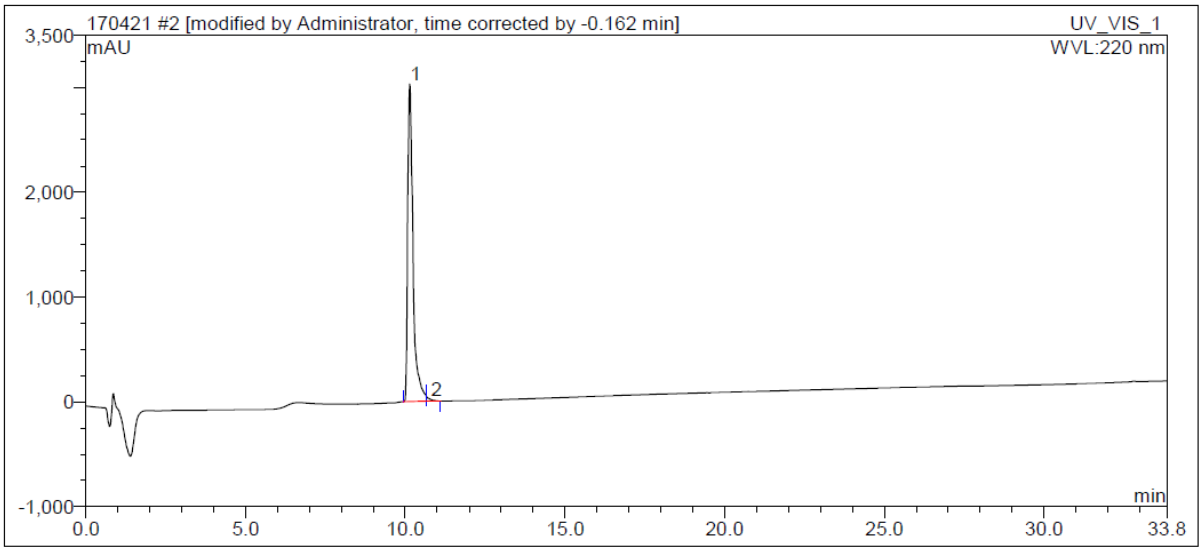

No.	Time	Area	Height	Rel.Area	
UV_VIS_1	UV_VIS_1 min	UV_VIS_1 mAU*min	UV_VIS_1 mAU	UV_VIS_1 %	
1	10.14	592.709	3032.355	98.76	product
2	10.80	7.460	16.435	1.24	

Certificate of analysis

peptides&elephants

www.peptides.de

Product	Pep2
Batch	0304Q02
ID	EP08327
Sequence	SWTWENGKWTWK-NH2
MW	1607.7

Identity

Peak #1

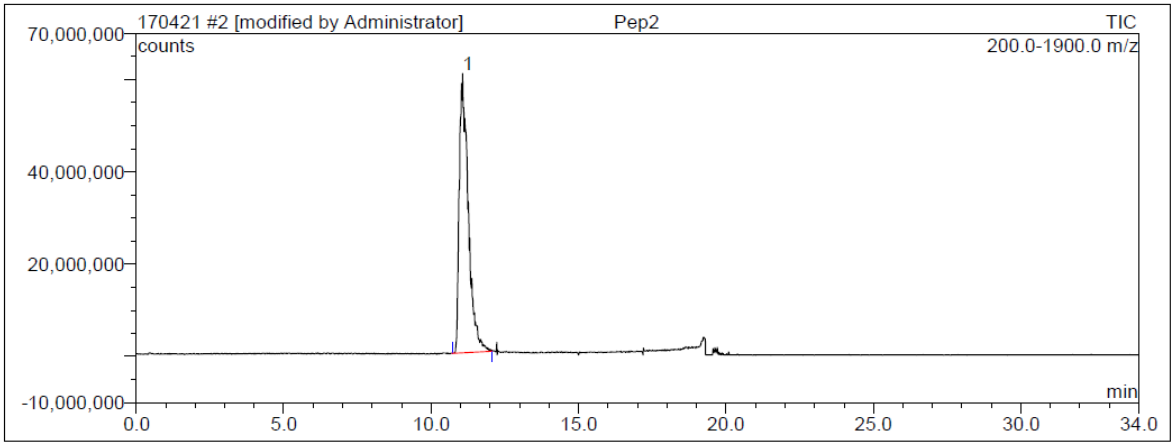

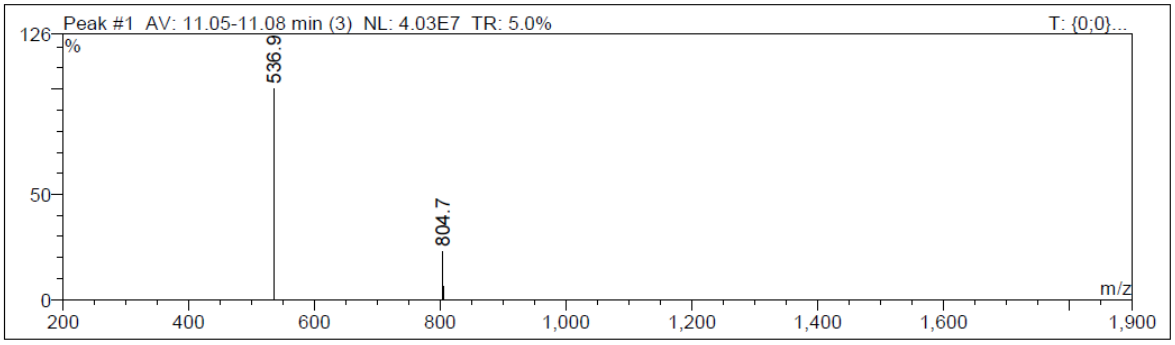

Mass m/z	Intensity counts	Relative Intensity %	found	calculated	Diff.	Test Resul	Charge
536.9	40272811	100.00%	1607.71	1607.73	0.02	passed	3
804.7	9135526	22.68%	1607.42	1607.73	0.31	passed	2

Trpzip-Q_2

Certificate of analysis

peptides&elephants

www.peptides.de

Product	Pep2
Batch	2702R04
ID	EP08328
Sequence	SWQWENGKWQWK-NH2
MW	1661.8

Purity

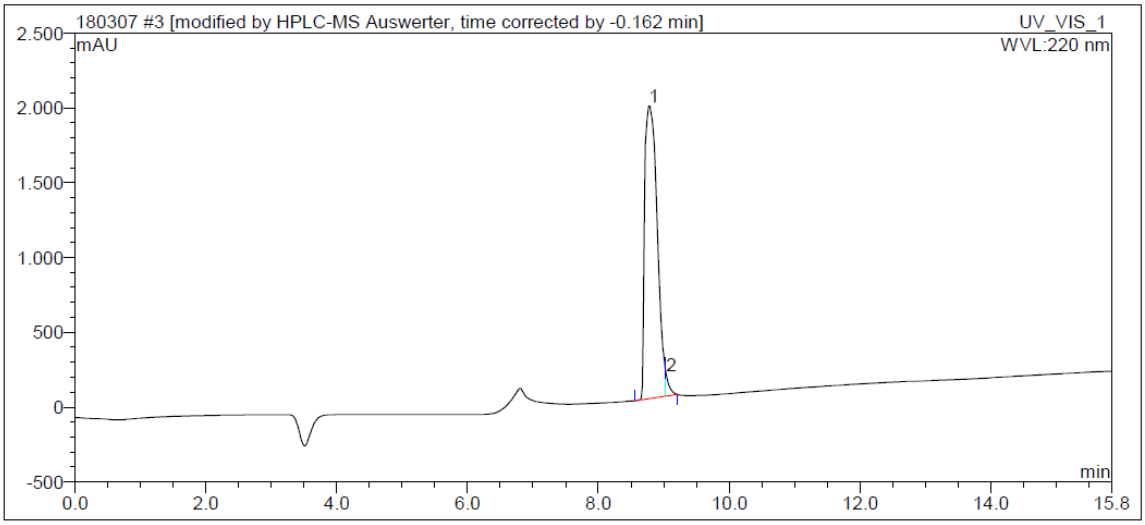

No.	Time	Area	Height	Rel.Area	
UV_VIS_1	UV_VIS_1 min	UV_VIS_1 mAU*min	UV_VIS_1 mAU	UV_VIS_1 %	
1	8.77	427.425	1956.502	97.70	product
2	9.04	10.057	143.036	2.30	

Certificate of analysis

peptides&elephants

www.peptides.de

Product	Pep2
Batch	2702R04
ID	EP08328
Sequence	SWQWENGKWQWK-NH2
MW	1661.8

Identity

Peak #1

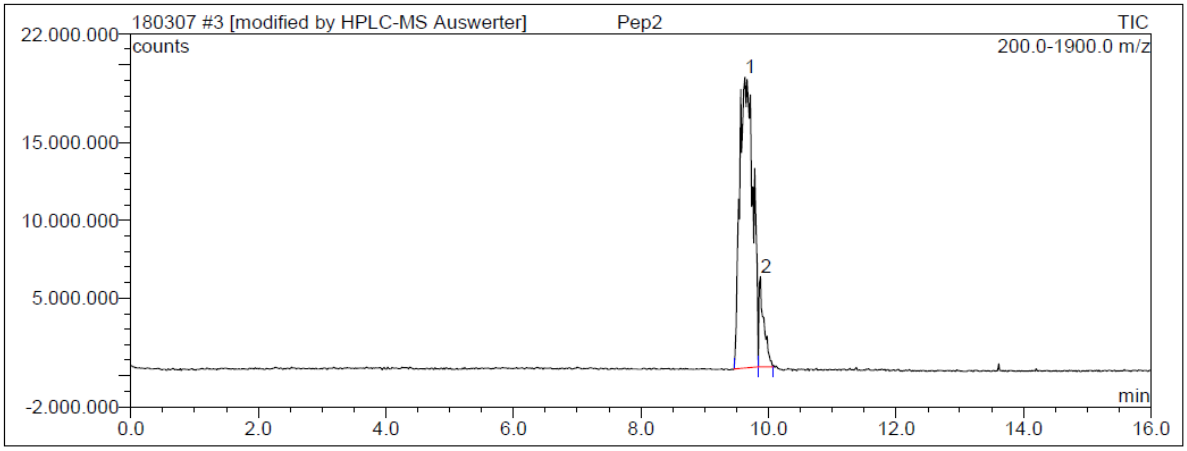

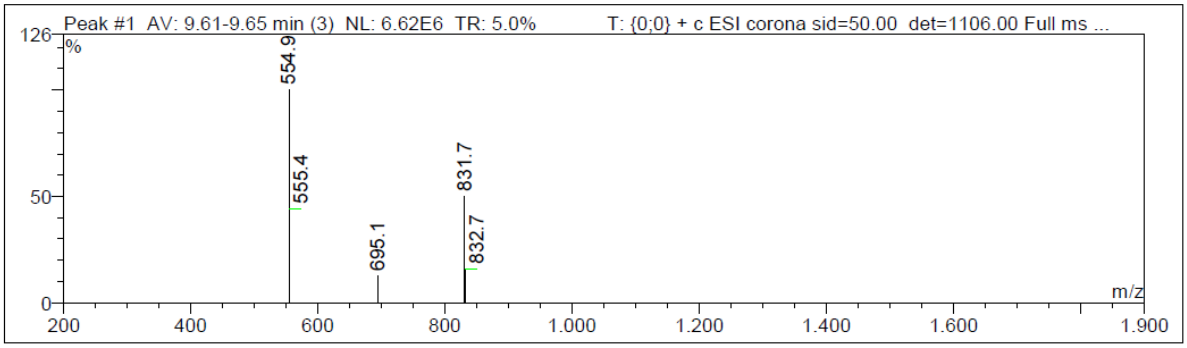

Mass m/z	Intensity counts	Relative Intensity %	found	calculated	Diff.	Test Resul	Charge
554.9	6619843	100.00%	1661.63	1661.8	0.17	passed	3
555.4	2927073	44.22%	1663.28	1661.8	-1.48	passed	3
695.1	827812	12.51%	1388.26	1661.8	273.54	failed	2
831.7	3312927	50.05%	1661.39	1661.8	0.41	passed	2
832.7	1050533	15.87%	1663.32	1661.8	-1.52	passed	2

Trpzip-Q_6

Certificate of analysis

peptides&elephants
www.peptides.de

Product	Pep3
Batch	2702R05
ID	EP09637
Sequence	SWQQQWENGKWQQQWK-NH2
MW	2174.3

Purity

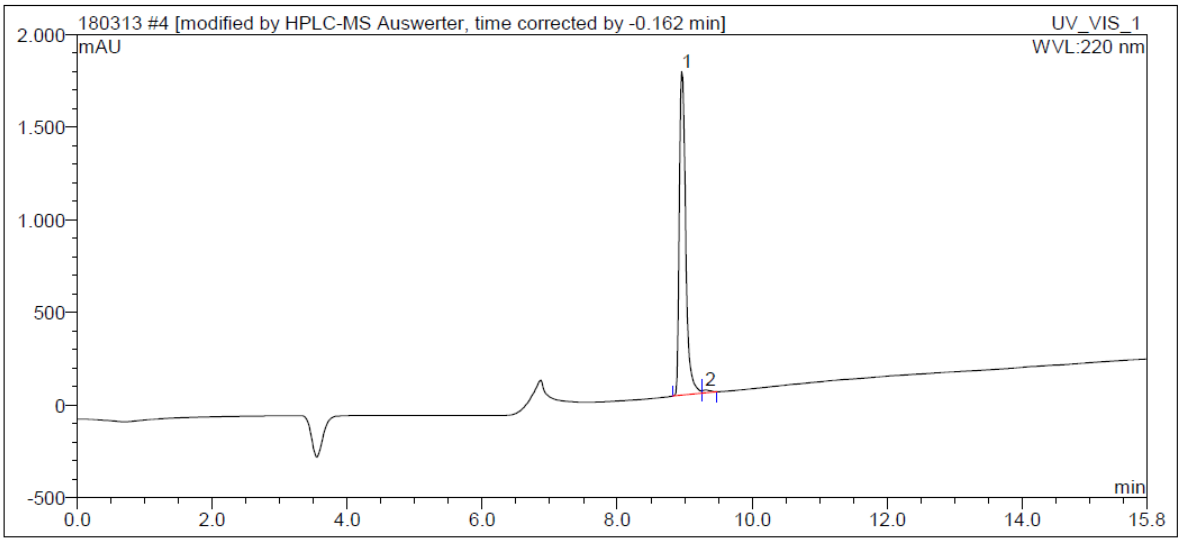

No.	Time	Area	Height	Rel.Area	
UV_VIS_1	UV_VIS_1 min	UV_VIS_1 mAU*min	UV_VIS_1 mAU	UV_VIS_1 %	
1	8.95	192.867	1747.963	99.00	product
2	9.30	1.952	16.122	1.00	

Certificate of analysis

peptides&elephants

www.peptides.de

Product	Pep3
Batch	2702R05
ID	EP09637
Sequence	SWQQQWENGKWQQQWK-NH2
MW	2174.3

Identity

Peak #1

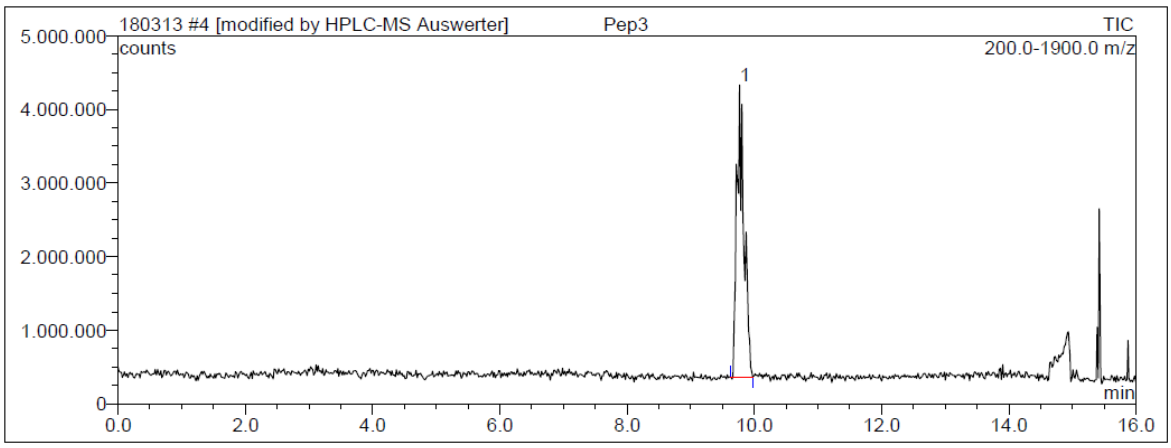

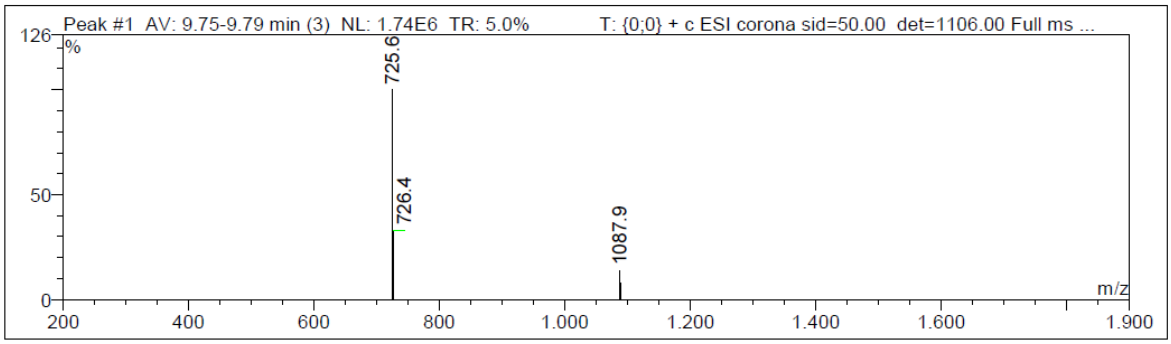

Mass m/z	Intensity counts	Relative Intensity %	found	calculated	Diff.	Test Resul	Charge
725.6	1737554	100.00%	2173.75	2174.31	0.56	passed	3
726.4	574168	33.04%	2176.25	2174.31	-1.94	passed	3
1087.9	242730	13.97%	2173.90	2174.31	0.41	passed	2

^{13}C isotopically labeled Trpzip-Q_6 (AWQ*Q*Q*WENGKWQ*Q*Q*WK-NH_2)

Certificate of analysis

peptides&elephants

www.peptides.de

Product	
Batch	0308P01
ID	EP06802
Sequence	AW-(1-13C)Gln-(1-13C)Gln-(1-13C)Gln-WENGKW(1-13C)Gln-(1-13C)Gln-(1-13C)Gln-WK-NH2
MW	2164.2

Purity

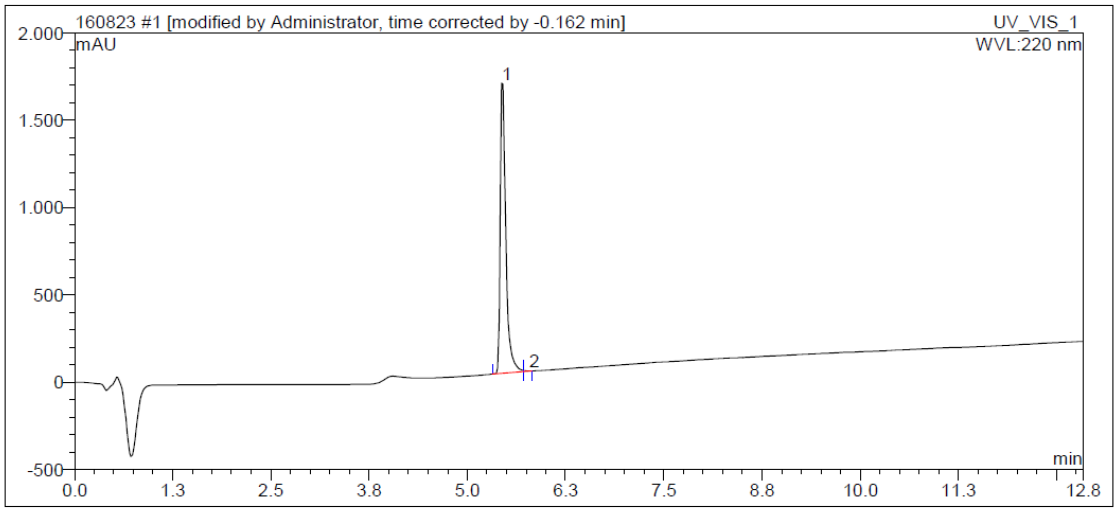

No.	Time	Area	Height	Rel.Area	
UV_VIS_1	UV_VIS_1 min	UV_VIS_1 mAU*min	UV_VIS_1 mAU	UV_VIS_1 %	
1	5.44	138.528	1661.596	99.84	Produkt
2	5.79	0.221	1.069	0.16	

Certificate of analysis

peptides&elephants

www.peptides.de

Product	
Batch	0308P01
ID	EP06802
Sequence	AW-(1-13C)Gln-(1-13C)Gln-(1-13C)Gln-WENGKW(1-13C)Gln-(1-13C)Gln-(1-13C)Gln-WK-NH2
MW	2164.2

Identity **Peak #1**

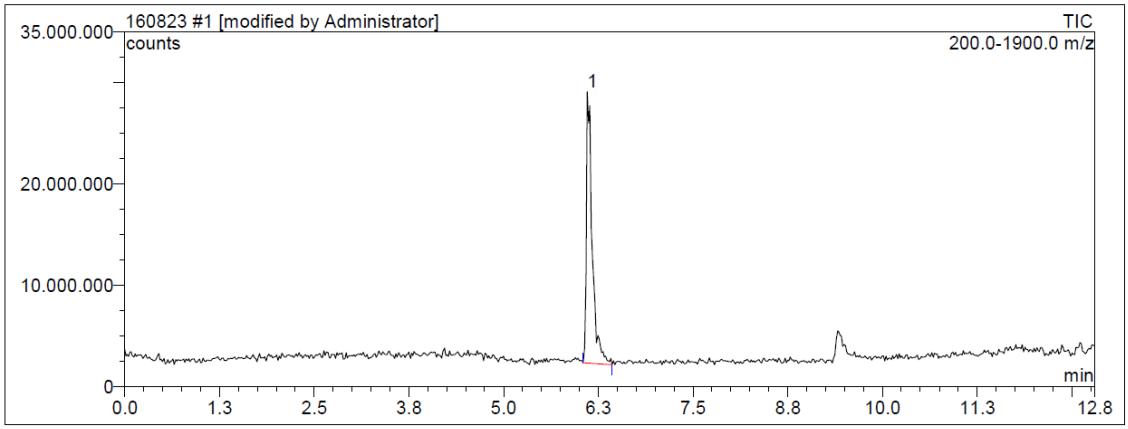

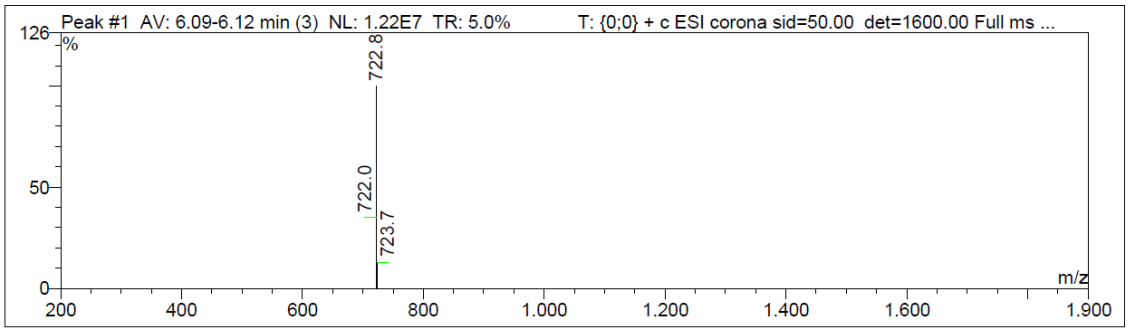

Mass m/z	Intensity counts	Relative Intensity %	found	calculated	Diff.	Test Resul	Charge
722.0	4292611	35.07%	2162.93	2164.2	1.27	passed	3
722.8	12241571	100.00%	2165.38	2164.2	-1.18	passed	3
723.7	1579097	12.90%	2167.99	2164.2	-3.79	passed	3

Trpzip-Q_{10}

Certificate of analysis

peptides&elephants

www.peptides.de

Product	Pep2
Batch	2203S03
ID	EP12910
Sequence	SWQQQQQWENGKWQQQQQWK-NH2
MW calc	2686.92

Purity

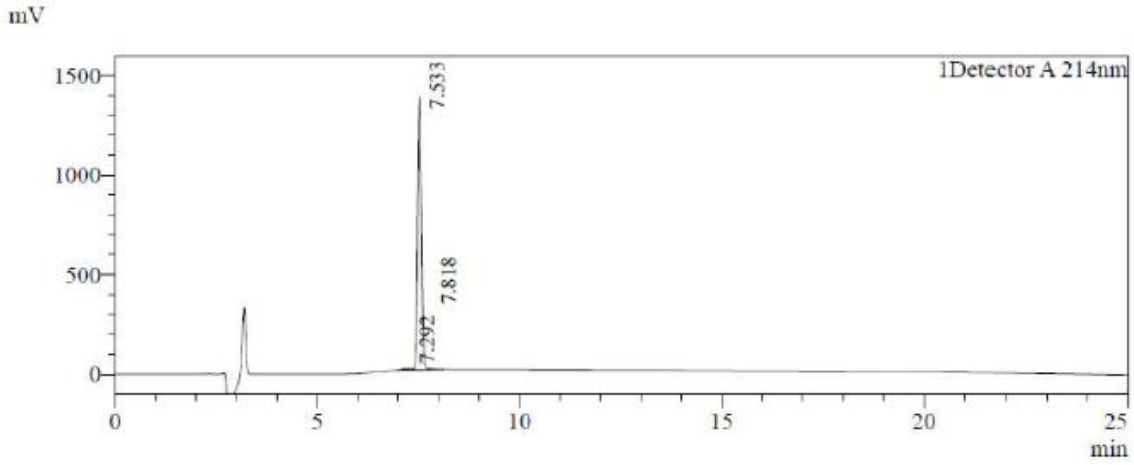

Peak Table

Detector A 214nm

Peak#	Ret. Time	Area	Height	Area%
1	7.292	109574	6388	1.265
2	7.533	8504614	1372666	98.145
3	7.818	51173	4869	0.591
Total		8665361	1383923	100.000

Certificate of analysis

peptides&elephants

www.peptides.de

Product	Pep2
Batch	2203S03
ID	EP12910
Sequence	SWQQQQQWENGKWQQQQQWK-NH2
MW calc	2686.92

Identity

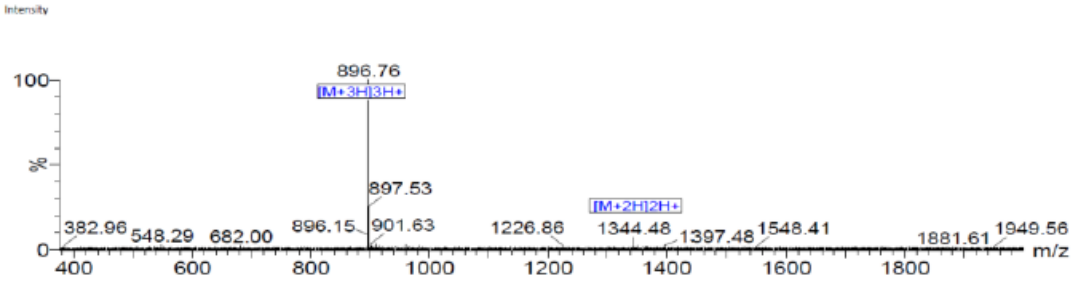

Trpzip-(QTQ)$_2$

Certificate of analysis

peptides&elephants

www.peptides.de

Product	Pep2
Batch	2008S05
ID	EP07432
Sequence	SWQTQWENGKWQTQWK-NH2
MW	2120.33

Purity

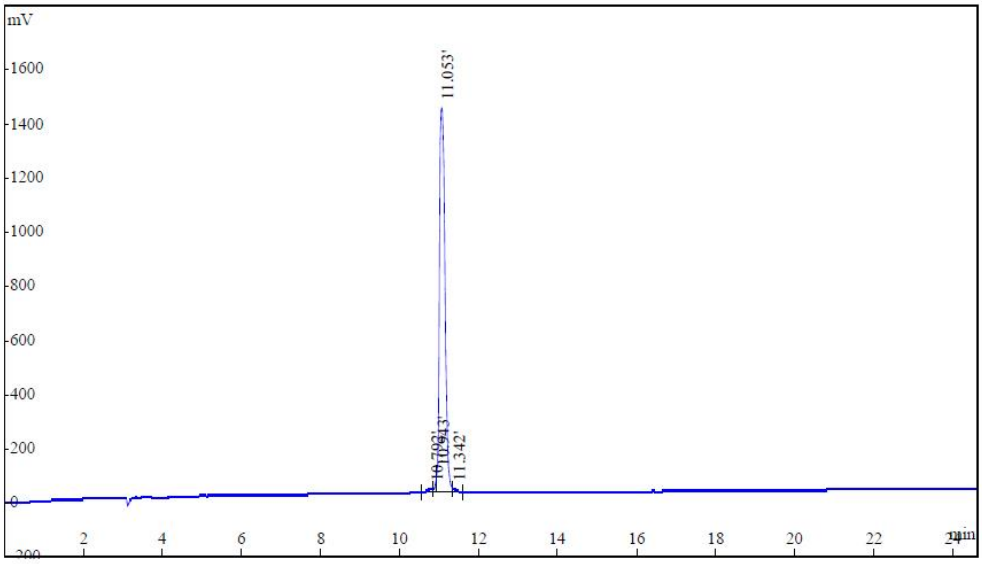

Rank	Time	Conc.	Area	Height
1	10.792	0.8281	105343	11103
2	10.943	1.4441	183695	69967
3	11.053	97.1404	12356546	1417729
4	11.342	0.5874	74713	12700
Total		100	12720297	1511499

Certificate of analysis

www.peptides.de

Product	Pep2
Batch	2008S05
ID	EP07432
Sequence	SWQTQWENGKWQTQWK-NH2
MW	2120.33

Identity

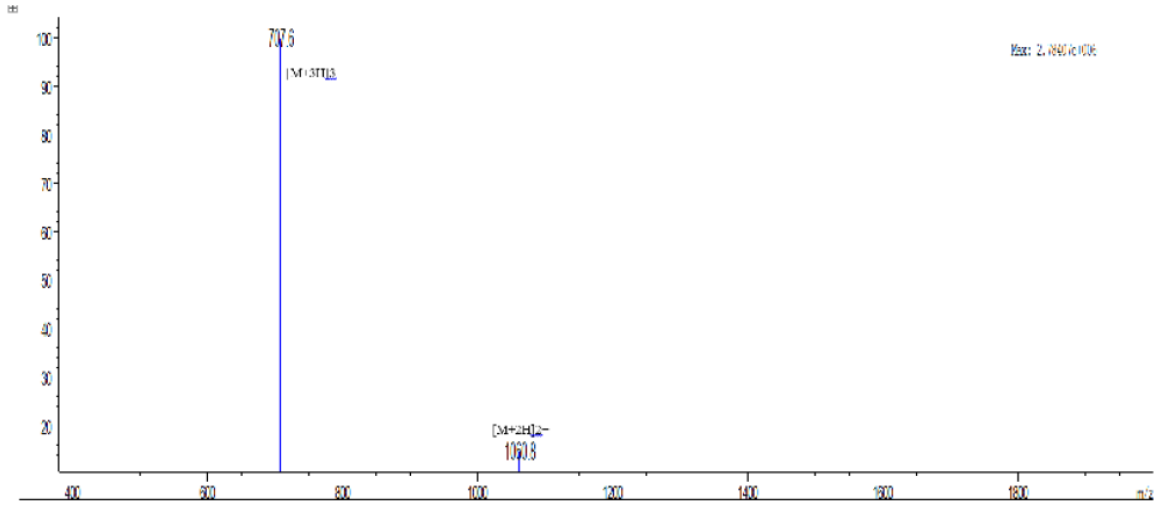

Trpzip-(QTQTQ)$_2$

Certificate of analysis

peptides&elephants

www.peptides.de

Product	Pep1
Batch	1702Q03
ID	EP08040
Sequence	SWQTQTQWENGKWQTQTQWK-NH2
MW	2578.8

Purity

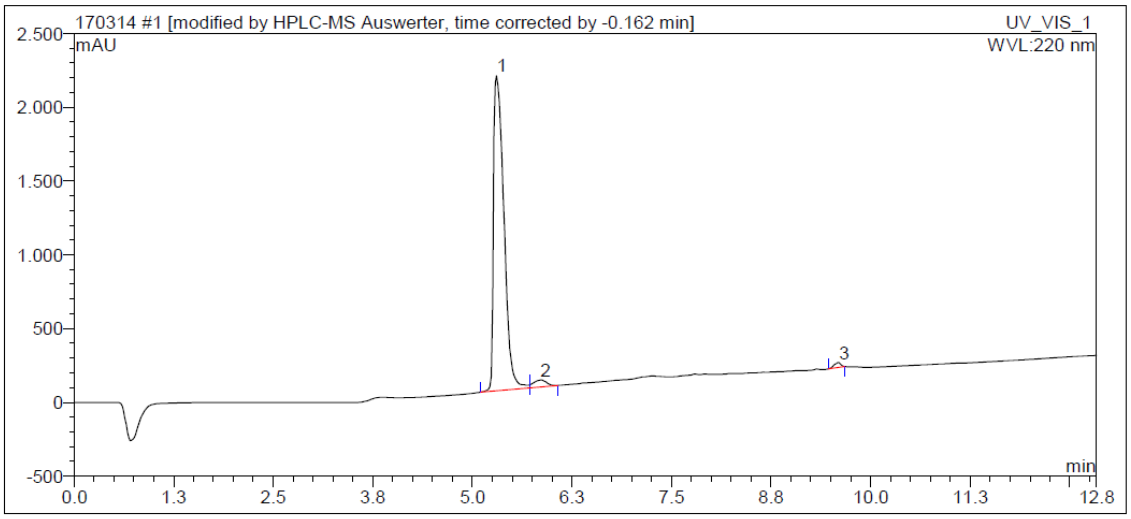

No. UV_VIS_1	Time UV_VIS_1 min	Area UV_VIS_1 mAU*min	Height UV_VIS_1 mAU	Rel.Area UV_VIS_1 %	
1	5.30	323.787	2135.048	96.44	Produkt
2	5.85	8.811	45.360	2.62	
3	9.60	3.127	32.963	0.93	

Certificate of analysis

peptides&elephants

www.peptides.de

Product	Pep1
Batch	1702Q03
ID	EP08040
Sequence	SWQTQTQWENGKWQTQTQWK-NH2
MW	2578.8

Identity

Peak #1

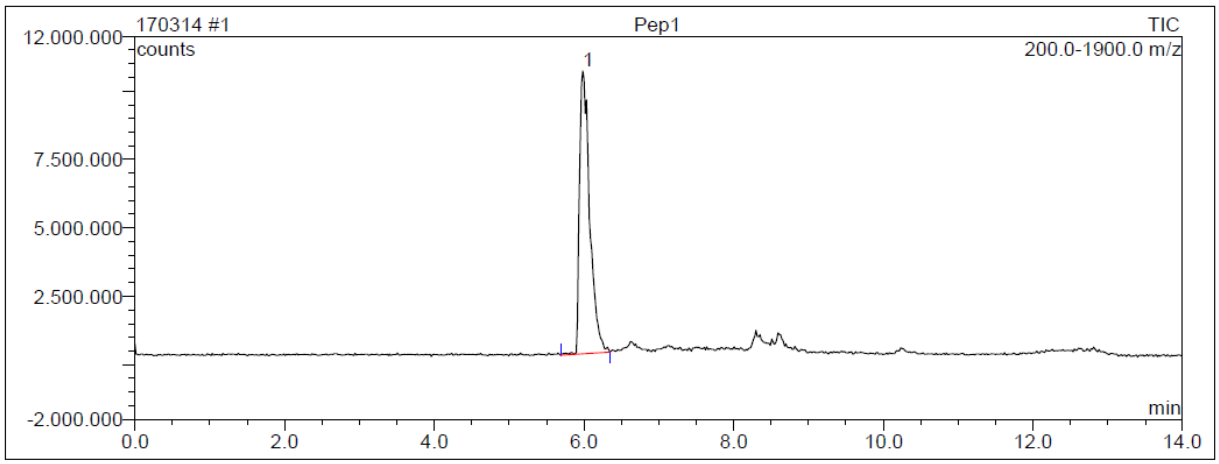

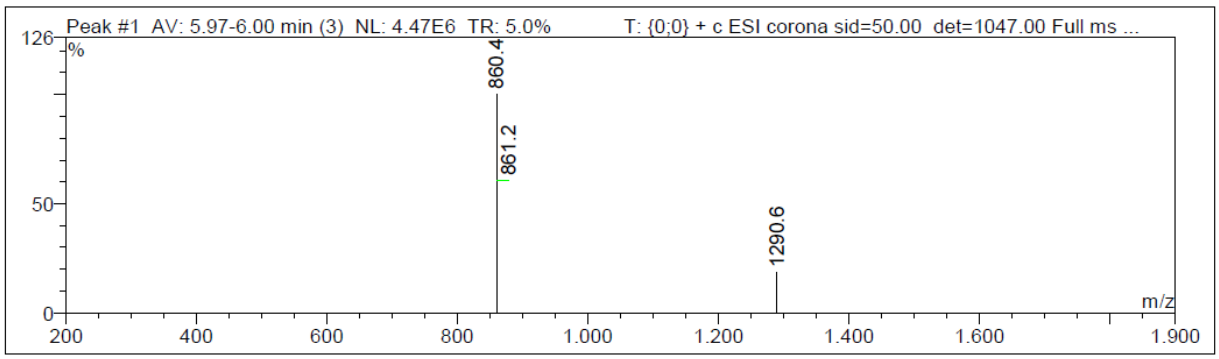

Mass m/z	Intensity counts	Relative Intensity %	found	calculated	Diff.	Test Resul	Charge
860.4	4471925	100.00%	2578.15	2578.8	0.65	passed	3
861.2	2702173	60.43%	2580.48	2578.8	-1.68	passed	3
1289.7	747848	16.72%	2577.47	2578.8	1.33	passed	2
1290.6	823898	18.42%	2579.11	2578.8	-0.31	passed	2

Trpzip-(QEQ)-(QKQ)

Certificate of analysis

peptides&elephants

www.peptides.de

Product	Pep3
Batch	2805S03
ID	EP08326
Sequence	SWQEQWENGKWQKQWK-NH2
MW calc	2175.41

Purity

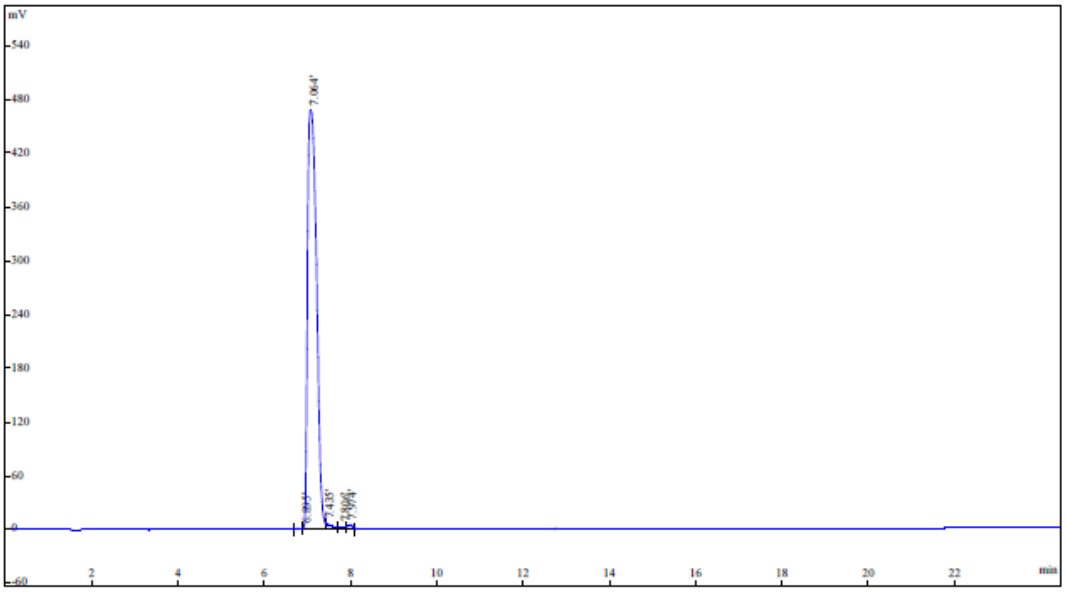

Rank	Time	Conc.	Area	Height
1	6.895	0.1444	9188	1233
2	7.064	98.17	6247774	466787
3	7.435	0.8088	51480	5318
4	7.806	0.3411	21707	2609
5	7.974	0.5385	34273	4612
Total		100	6364422	480559

Certificate of analysis

peptides&elephants

www.peptides.de

Product	Pep3
Batch	2805S03
ID	EP08326
Sequence	SWQEQWENGKWQKQWK-NH2
MW calc	2175.41

Identity

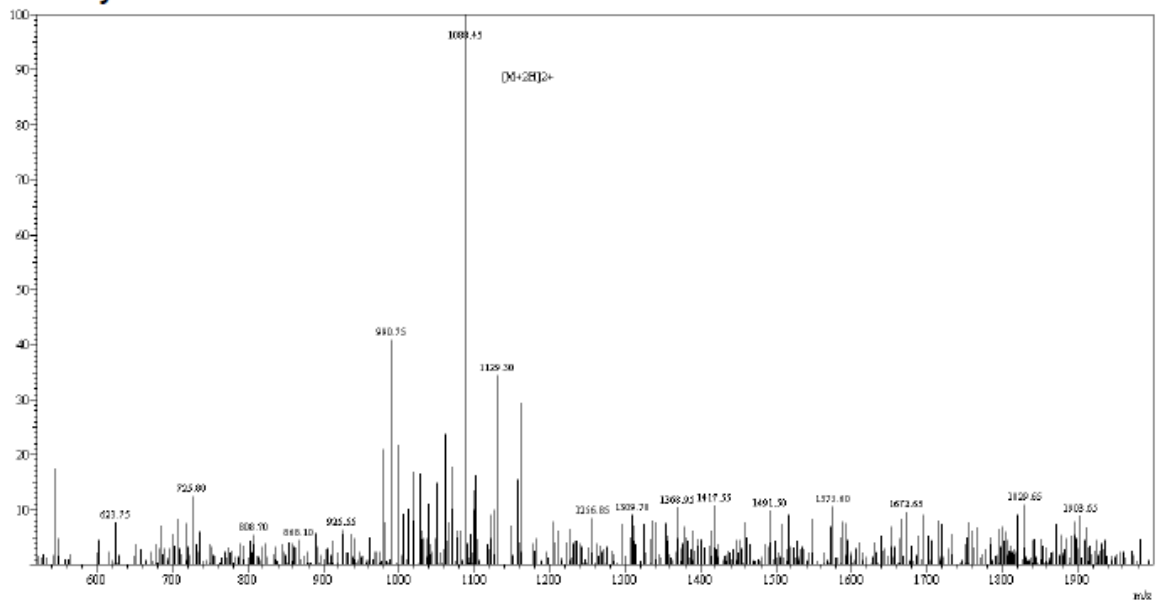

Trpzip-(QEQKQ)$_2$

Certificate of analysis

www.peptides.de

Product	Pep2
Batch	1311Q02
ID	EP09131_1
Sequence	SWQEQKQWENGKWQEQKQWK-NH2
MW	2688.97

Purity

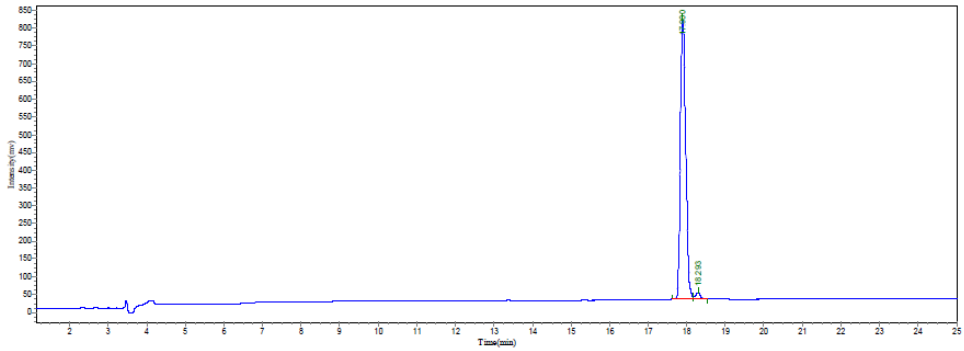

Peak No.	Ret Time	Height	Area	Conc.
1	17.900	786405.375	7675743.500	97.9472
2	18.293	17177.318	160873.063	2.0528
Total				100.0000

Certificate of analysis

www.peptides.de

Product	Pep2
Batch	1311Q02
ID	EP09131_1
Sequence	SWQEQKQWENGKWQEQKQWK-NH2
MW	2688.97

Identity

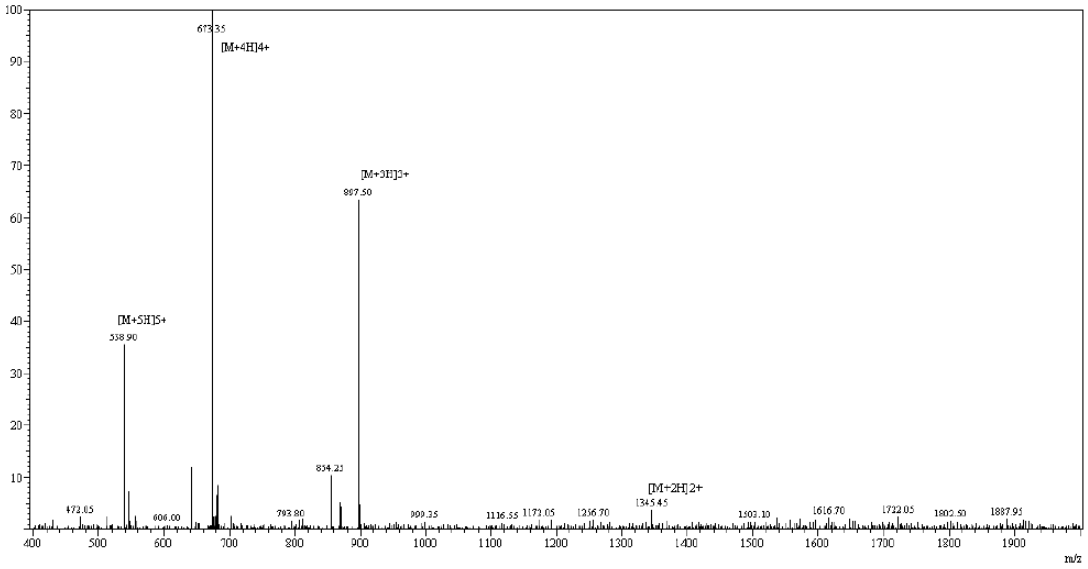

Trpzip-(QWQW)-(WQWQ)

Certificate of analysis

peptides&elephants

www.peptides.de

Product	Pep5
Batch	2805S05
ID	EP13108
Sequence	SKQWQWENGKWQWQEK-NH2
MW calc	2175.41

Purity

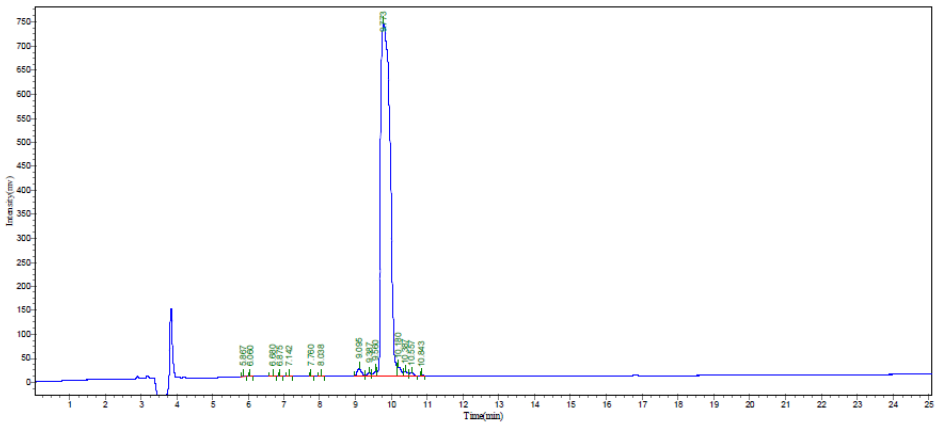

Peak No.	Ret Time	Height	Area	Conc..
1	5.867	649.739	3334.396	0.0249
2	6.060	278.261	1073.597	0.0080
3	6.680	908.475	5676.801	0.0424
4	6.875	263.619	1359.999	0.0102
5	7.142	465.346	2577.595	0.0192
6	7.760	280.494	1247.999	0.0093
7	8.038	943.223	5217.610	0.0389
8	9.095	14342.529	117238.094	0.8751
9	9.387	4465.857	39235.441	0.2929
10	9.560	9202.530	60850.828	0.4542
11	9.773	735083.813	12929859.000	96.5084
12	10.180	18722.238	118265.023	0.8827
13	10.387	8892.966	70234.094	0.5242
14	10.557	4958.204	36533.293	0.2727
15	10.843	1087.229	4953.592	0.0370
Total				100.0000

Certificate of analysis

peptides&elephants

www.peptides.de

Product	Pep5
Batch	2805S05
ID	EP13108
Sequence	SKQWQWENGKWQWQEK-NH2
MW calc	2175.41

Identity

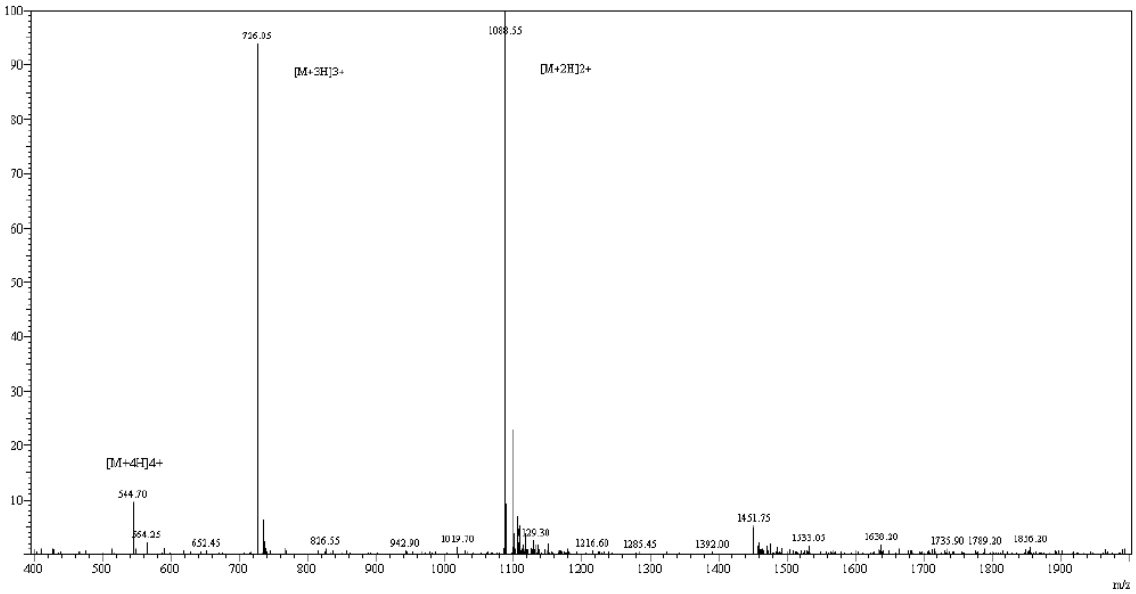

References

1. D. K. Wilkins, S. B. Grimshaw, V. Receveur, C. M. Dobson, J. A. Jones and L. J. Smith, Hydrodynamic radii of native and denatured proteins measured by pulse field gradient NMR techniques, *Biochemistry*, 1999**, 38** (50), 16424-16431.
2. D. M. John and K. M. Weeks, Van't Hoff enthalpies without baselines, *Protein Science*, 2000, **9** (7), 1416-1419.